

https://dspace.org/

Design and evaluation of an oral 3D printed chemotherapeutic delivery system

Clark, Karin

2021
https://hdl.handle.net/10539/33496

Downloaded from a DSpace repository. https://dspace.org/

DESIGN AND EVALUATION OF AN ORAL 3D PRINTED CHEMOTHERAPEUTIC DELIVERY SYSTEM

KARIN CLARK

A dissertation submitted to the Faculty of Health Sciences, University of the Witwatersrand, in fulfilment of the research requirements for the degree of Master of Science in Medicine: Pharmaceutical Affairs



Supervisors:

Professor Pierre P. D. Kondiah, Professor Yahya E. Choonara and Professor Viness Pillay,

Department of Pharmacy and Pharmacology, Faculty of Health Sciences,

University of the Witwatersrand, South Africa

Johannesburg

2021

DECLARATION

I Karin Clark declare that this Research Report is my own work. It is being submitted for the Degree Master of Science in Medicine: Pharmaceutical Affairs at the University of the Witwatersrand, Johannesburg. It has not been submitted before for any degree or examination at any other University.

(Signature of candidate)

14 day of September 20 21 in Reigate, United Kingdom

ABSTRACT

Cancer is one of the prevalent diseases that continues to give physicians, scientists and researchers challenges in the delivery of oral chemotherapeutic agents. Conventional chemotherapeutics with fixed doses may lead to minimal concentrations reaching cancer targeted sites that are severe. Nanoparticles (NPs) are used as drug carriers that offers many advantages in chemotherapeutics such as targeted therapy, controlled release, increased stability, increased shelf life and high carrier capacity. Three-dimensional (3D) printing further offers a unique solution to the several limitations in cancer patients. 3D printing can print biodegradable oral delivery systems which can be customised to patients. This study aimed to design and develop a novel drug delivery system employing methotrexate-loaded nanoparticles encapsulated in alginate-gelatine 3D printable ink hydrogel to form a solid 3D printed tablet for oral chemotherapeutic delivery. A biodegradable polymeric nanoparticulate system was formulated using d-α-Tocopheryl polyethylene glycol 1000 succinate (TPGS) and poly (lactic-co-glycolic acid) (PLGA) for methotrexate (MXT) entrapment. The oral chemotherapeutic tablet was then formed using the 3D bioplotter from nanoparticle formulation incorporated with sodium alginate-gelatine hydrogel ink. Fourier-transform infrared spectroscopy (FTIR), Scanning Electron Microscopy (SEM), and Thermal Gravimetric Analysis (TGA) confirmed polymer combinational synthesis of MTX polymeric nanoparticles. The MTX polymeric nanoparticles were 186 nm in size, with a zeta potential of -31.4 mV, (PDI ≤ 0.5), and a percent drug entrapment efficiency (DEE%) value of >85%. The SEM indicated that MTX polymeric nanoparticles were well distributed and had a regular orbicular shape. FTIR displayed comparable peaks to PLGA and MTX displaying MTX polymeric nanoparticle's similar chemical composition suggesting that there was no significant chemical interaction between the functional groups of MTX and PLGA during formation of the nanoparticles. Overall, results demonstrated that the MTX polymeric nanoparticles were successfully synthesized. The results also indicated that the high accuracy of the 3D printed hydrogel/nanocomposite system (including 15 sec pauses between layers) was achieved using a 25 G needle with inner diameter of 25 mm, optimal printing pressure was1400 kPa and 95% printing accuracy. The 3D Bioplotter parameters were optimised and validated. The oral 3D printed hydrogel/nanocomposite system for the targeted delivery of methotrexate was produced. *In vitro* drug release profiles were investigated at pH 7.4 and pH 1.2 to simulate the gastrointestinal environment. The *in vitro* release profile of MTX loaded nanoparticles displayed constant release of MTX over 24 hours. The development of this 3D printed drug delivery tablet

may have potential to overcome the chemotherapeutic challenges experienced with conventional therapies.

TABLE OF CONTENTS

DECLARATION ii
ABSTRACT iii
LIST OF FIGURES viii
LIST OF TABLES ix
LIST OF ABBREVIATIONS x
CHAPTER 1 1
1.1 Introduction and Background on Cancer and treatment 1
1.2 Rationale and Motivation of the Study 3
1.3 Aim and objectives of this study 4
1.4. Overview of the Dissertation 4
CHAPTER 2 6
2.1 Introduction 6
2.2 Oral drug delivery 7
2.3 Methotrexate nanoparticles in cancer treatment 10
2.4 Nanocomposite hydrogels as 3D printable inks for advanced drug delivery 11
2.5 3D Printing: State-of-the Art in Drug Delivery Systems Design 12
2.5.1 Methods of 3D Printing 14
2.5.2 Limitations of 3D Printing in Chemotherapeutic Drug Delivery 15
2.6 Concluding Remarks 15
CHAPTER 3 17
3.1 Introduction 17
3.2 Methods and Materials 18
3.2.1 Materials 18
3.2.2 Preparation of Methotrexate-loaded TPGS-PLGA nanoparticulate system 18
3.2.3 Componential analysis of chemical structure integrity post nanoparticle formation 19
3.2.4 Nanomiretic characterization of the MTX-loaded TPGS-functionalized PLGA nanoparticles 19
3.2.5 SEM Characterisation of MXT-loaded TPGS-PLGA nanoparticles 19
3.2.6 Thermal analysis Methotrexate-loaded TPGS and PLGA nanoparticles. 20
3.2.7 *In vitro* evaluation of Methotrexate release from the TPGS-PLGA nanoparticles. 20
3.3 Results and Discussion 20
3.3.1 Assessment of MTX-loaded TPGS-functionalized PLGA nanoparticles 20
3.3.2 Assessment of MTX-loaded TPGS-functionalized PLGA nanoparticles thermal stability 24

3.3.3 Evaluation of the chemical stability and integrity of the various nanosystem components 27
3.3.4 Drug Release Kinetics of Methotrexate from TPGS and PLGA nanoparticles 28
3.4 Concluding Remarks 28
CHAPTER 4 30
4.1 Introduction 30
4.2. Materials and Methods 31
4.2.1 Materials 31
4.2.2 Optimisation of Printing Parameters 31
4.2.3 Printability and optimisation of Sodium Alginate Gelatine Bio-ink 32
4.2.4 Optimum Hydrogel printable ink of Sodium Alginate/ Gelatine 32
4.2.5 Determination of the effect of needle gauge on 3D printing accuracy 32
4.2.6 Crosslinking of sodium alginate 33
4.2.7 Temperature induced Crosslinking of Gelatine 33
4.2.8 Determination of optimum printing speed and pre- and post-flow delay times 34
4.3 Results and Discussion 34
4.3.1 Optimisation of Sodium Alginate/ Gelatine Printing Ink 34
4.3.2 The influence of printing needle size on 3D printing accuracy 35
4.3.3 Optimisation of crosslinking time of Sodium Alginate-Gelatine devices in $CaCl_2$ 36
4.3.4 Determination of optimum printing temperature 36
4.3.5 The influence of printing speed and pre- and post-flow dwell times on 3D printing accuracy 37
4.3.6 The influence of temperature on 3D printing accuracy 37
4.3.7 Optimisation of the ionic crosslinking time of SA-GL matrices 38
4.4 Concluding Remarks 38
CHAPTER 5 39
5.1 Introduction 39
5.2 Methods 40
5.2.1 Materials 40
5.2.2 Preparation of Sodium Alginate-Gelatine Nanoparticle Formulation Printing Ink 40
5.2.3 Design of 3-D Printed Tablets 40
5.2.4 Thermal Analysis of 3D Printed Tablets 41
5.2.5 *In Vitro* Analysis of the 3D Printed Sodium Alginate-Gelatine Hydrogel- Nanoparticle Formulation for Oral Drug Delivery 41
5.3 Results and Discussion 42

5.3.1. 3-D Printing of Sodium Alginate-Gelatine Hydrogel Nanoparticle Formulation (Oral Chemotherapeutic Delivery System) 42
5.3.2. Determination of thermal stability of the Sodium Alginate-Gelatine Nanoparticle Formulation 42
5.3.3 Drug release profiles of the Sodium Alginate-Gelatine Hydrogel Nanoparticulate system 44
5.4 Concluding Remarks 45
CHAPTER 6 46
6.1 Conclusion 46
6.2 Future Recommendations 47
REFERENCES 49

LIST OF FIGURES

Figure 2. 1 Schematic overview of main drug transporters expressed on enterocytes in intestinal epithelia membrane: P-glycoprotein (Pgp); multidrug resistance-associated protein 1 (MRP1); multidrug resistance-associated protein 2 (MRP2); breast cancer resistance protein (BCRP) (Sohail, et al., 2018) 8

Figure 3. 1 Particle size distribution profile of Methotrexate-loaded polymeric TPGS-PLGA nanoparticles (nanoparticle formulation). 21

Figure 3. 2 Distribution profile of Zeta Potential of the Methotrexate-loaded TPGS-PLGA nanoparticles (nanoparticle formulation). 22

Figure 3. 3 Gold-platinum sputtered SEM Micrograph of Methotrexate-loaded TPGS-PLGA nanoparticles. (A) Magnification = 15.84 KX; Voltage =6.00 kV (B) Magnification = 44.34 KX; Voltage =6.00 kV. SEM of optimized Methotrexate loaded nanoparticle formulation showing sphericity, smooth surface of nanoparticles. 23

Figure 3. 4 (A) TGA curves of methotrexate (MXT). (B) TGA curves of blank PLGA nanoparticles. (C) TGA curves of the Methotrexate-loaded in polymeric TPGS-PLGA nanoparticle. 24

Figure 3. 5 (A) DSC curves of methotrexate (MXT). (B) DSC curves of blank PLGA nanoparticles. (C) DSC curves of the Methotrexate-loaded in polymeric TPGS-PLGA nanoparticle. 26

Figure 3. 6 (A) FTIR spectra of methotrexate (MXT). (B) FTIR spectra of PLGA-TPGS. (C) FTIR spectra of Methotrexate-loaded in polymeric TPGS-PLGA nanoparticles (nanoparticle formulation). (D) FTIR spectra of TPGS. 28

Figure 3. 7 In vitro release of MXT from TPGS-PLGA nanoparticles at a stomach acidity of pH 1.2 and intestinal environment of pH 7.4 (n=3, mean ± SD) 28

Figure 4. 1 Image (A) and schematic diagram (B) of 3D-Bioplotter, a versatile rapid prototyping tool (Naghieh, 2018). 31

Figure 4. 2 Sodium alginate gelation through crosslinking by exchange of sodium ions (Na+) and calcium ions (Ca^{2+}). 33

Figure 4. 3 Images of typical 3D printed SA-GL tablet-shaped matrices produced using a 3D Bioplotter in the least and most favourable concentrations: a. Least favourable printing ink (5%SA-8%GL) and b. Most accurate printing ink (8%SA-10%GL) 35

Figure 4. 4 Dried 3D printed sodium alginate-gelatine hydrogel devices following temperature and chemical crosslinking in $CaCl_2$ 38

Figure 5. 1 Thermogravimetric (TGA) analysis of Sodium Alginate-gelatine printing ink (as prepared; prior to 3D printing and; thermal and chemical crosslinking) 43

Figure 5. 2 Thermogravimetric (TGA) analysis of 3D Printed Sodium Alginate-Gelatine Nanoparticle Formulation (Oral Chemotherapeutic Delivery System). 44

Figure 5. 3 In vitro MTX release from Sodium Alginate-Gelatine Nanoparticle Formulation conducted in pH 1.2 and pH 7.4 buffer (n=3, mean ± SD) 45

LIST OF TABLES

Table 4. 1 Printing accuracy of different concentrations of Sodium Alginate/ Gelatine in printing ink. 34
Table 4. 2 Assessment of 3D printing needle size and printing accuracy (%) of matrices 35
Table 4. 3 Extrudability of printing ink at different temperatures 36
Table 4. 4 Influence of 3D printing speed on printing accuracy 37

LIST OF ABBREVIATIONS

3D	Three-Dimensional
CYP450	Cytochrome P450
FDA	Food and Drug Administration Organisation
FDM	Fused Deposition Modelling
FTIR	Fourier-Transform Infrared Spectroscopy
MTX	Methotrexate
NP	Nanoparticle
PDI	Particle Dispersion Index
PEG	Poly (Ethylene Glycol)
P-gp	Efflux Protein P-Glycoprotein
PLGA	Poly (Lactic-Co-Glycolic Acid)
PVPA	vesicle-based permeation assay
SAG	Sodium Alginate - Gelatine
SEM	Scanning Electron Microscopy
SLS	Selective Laser Sintering
TGA	Thermogravimetric Analysis
TPGS (1000)	D-A-Tocopheryl Polyethylene Glycol 1000 Succinate
OC	ovarian cancer
UV-Vis	Ultraviolet–visible spectroscopy
WHO	World Health Organisation

CHAPTER 1
INTRODUCTION

1.1 Introduction and Background on Cancer and treatment

According to the World Health Organisation (WHO), cancer is the second leading cause of death globally, accounting for nearly 9.6 million deaths recorded at the end of 2018. The main goal of cancer diagnosis and treatment programmes are to cure or considerably prolong the life of patients and to ensure the best possible quality of life for cancer survivors (WHO, Cancer). Seabury et al. (2018) conducted a study to determine the effect of cancer treatment on work productivity and healthcare utilization, among patients with breast and lung cancer. They found that when compared to intravenous docetaxel chemotherapy, a treatment modality that could be self-administered was associated with a reduction in both the number and length of sick days taken and with fewer outpatient services visits.

When it comes to the administration of medications, oral administration is preferable to injectable treatment. Oral administration of medication is associated with better patient compliance, is more economical and is better tolerated in chronic treatment regimens. (Yang, Zhang and Liang). Oral administration is generally convenient, painless, and safe, and therefore preferred by the patients. In addition, oral formulations are easy to store and transport (Du et al., 2018). Nevertheless, solid dosage oral medications that are mass-produced in predefined strengths have several disadvantages. Providing an extremely diverse world population with limited doses can result in patients receiving higher or lower doses than required, causing either adverse effects or inadequate therapeutic levels (Alomari et al., 2015). These dosing limitations are particularly relevant for cancer patients, where the treatment is usually associated with severe adverse events and need for adequate therapeutic levels. It is therefore urgent to develop a new oral formulation to avoid the severe side effects without an obvious reduction in the drug efficacy of cancer medication (Yang et al., 2015). Unlike conventional manufacturing processes, 3D printing offers a unique option to produce patient-customised oral delivery systems (Kyobula, Adedeji and Alexander).

Other challenges associated with oral administration includes poor aqueous solubility, poor enzymatic stability, gastrointestinal pH and efflux pumps that are located in gastrointestinal (Desai, 2012). Therefore, there is an urgent need to develop new oral nanoformulation to

overcome aforementioned challenges without reduction in drug efficacy of cancer medication (Yang et al., 2015).

To support the design of new oral chemotherapeutic formulations, advances in nanotechnology could play a pivotal role in the control of drug release, targeting and drug stability. Nanoparticles (NPs) as drug carriers have several advantages, which include increased stability, enhanced increased shelf life, and high drug carrier capacity (Pawar , Singh and Sharma). Nanoparticles are defined as submicron colloidal particles in which the drug is absorbed, dissolved, or dispersed throughout the matrix and nanocapsules, in which the drug is confined to an aqueous or oily core surrounded by a shell-like wall (Maksimenko, Malinovskaya and Shipulo). Wang et al., 2013 theorized that the d-α-Tocopheryl polyethylene glycol 1000 succinate (TPGS) shows effective toxicity for cancer cells and thus could synergistically enhance the therapeutic efficacy of drug-loaded TPGS-containing nanoparticles. Liang, et al., 2010 reviewed the use of nanotechnology to prevent tumour resistance to chemotherapy and found that nanoparticles are an effective strategy for overcoming drug resistance in cancer cells (Liang, Chen and Zhao). Several factors determine the cellular uptake of nanoparticles. These factors include size, surface functionalisation and surface hydrophobicity/hydrophilicity. Nanoparticle size is an important component in the process of cellular uptake as it directly influences the endocytotic route. Nanoparticles with a size of less than 200 nm are internalized via clathrin- or caveolin-mediated endocytosis and thereby avoid expulsion by the reticuloendothelial system. In addition, more than 30 years poly lactic-co-glycolic acid (PLGA) has been seen as polymeric candidates of choice for drug delivery and tissue engineering applications (Siegel, Poly Lactic-co-Glycolic Acid (PLGA) as Biodegradable Controlled Drug Delivery Carrier). PLGA is biocompatible and biodegradable material that can be used to nanoformulate chemotherapies. Solid dosage medications are mass-produced in predefined strengths, however, have several disadvantages such as fixed dose regardless of severity of cancer in each individual and this results in patients receiving higher or lower doses than required causing either adverse effects or inadequate therapeutic levels (Alomari et al., 2015). The alternative strategy may be the 3D bio-printing technology due to specific doses of nanoformulated chemotherapeutic agent that are loaded in sodium alginate gelatine bio-ink printed and administered as customised oral delivery systems (Kyobula et al., 2017).

Methotrexate (MTX) is used as an antimetabolite in cancer chemotherapy. MTX has an essential role in the treatment of diverse illnesses such as breast cancer, acute lymphocytic leukemia,

osteosarcoma, non-Hodgkin's lymphoma, choriocarcinoma, head and neck cancer (Jolivet, 1983) MTX is dosed orally, intramuscular and intravenous depending on the type of cancer and also doses varies based on age and severity of cancer. Paxton et al., 1981 conducted a study evaluating protein binding of MTX and found that 46.5 ± 2.7% binds in plasma proteins (Paxton, 1981). Instability of active compounds leads to substantial lower quantity of the dosage, for instance MTX undergoes alkaline hydrolysis reaction at alkaline pH and form N-methylfolic acid (Sayantan Ray). It is essential that drug delivery system designed enhances active compound stability and minimise by-products that can introduce toxicity.

1.2 Rationale and Motivation of the Study

Oral administration of medication is generally preferred by the patients due to the convenience, lack of invasive procedures and safety, however solid dosage oral medications that are mass-produced in predefined strengths have several disadvantages for cancer patients, where there is a very fine balance between toxicity and efficacy. (Yang, Zhang and Liang). Additionally, dosing requirements in paediatric and geriatric patients can be significantly different to normal patient doses. This is due to variations in pharmacokinetics and presents a problem when medicines are manufactured at a specific strength or formulation type. Often, the medications are then split or crushed to obtain the required dose, which could lead to incorrect dosing or dose dumping (premature and exaggerated release of a drug) (Alomari et al., 2015). Personalised medicine can be used to create patient's specific doses to prevent over- or under dosing of patients as well as reduce side effects. The use of 3D printers in pharmaceutical production has demonstrated great potential as an alternative technique for personalising dosage forms (Okwuosa et al., 2018). A study undertaken by Musmade et al., 2014 showed that MTX-loaded PLGA nanoparticles prepared by emulsification solvent evaporation method released the MTX slowly and increased the retention time in the cells as compared to free MTX. The NPs had an initial burst release of MTX followed by a long period of sustained release. *In vitro* cytotoxicity assays conducted also demonstrated that cancer cell death is significantly increased with MTX-loaded nanoparticles compared to free MTX (Musmade et al., 2014). Combining nanoparticles with hydrogels for 3D printing of oral drug delivery devices provides an excellent solution. Hydrogels are hydrophilic, complex polymeric networks which are able to absorb large quantities of organic fluids. Hydrogels resemble natural living tissue due to their capability of excessive fluidic content, porosity and tender consistency (Lynch, et al., 2020). Cross-linked hydrogel networks can protect drugs from harmful environments, such as enzymes and low pH in the stomach (Qiu, et al., 2001). Hydrogels

are stable and may gradually degrade, disintegrate and dissolve inside the biological system. The study conducted by Beck et al. (2017) was the first attempt to conjugate nanotechnology and 3D printing. In this study, polymeric nanocapsules were successfully loaded in fused deposition modelling (FDM) printed devices prepared from printable polymeric filaments. The concepts used in this study can be used to develop patient-tailored dose and drug release dosage forms of oral medication.

1.3 Aim and objectives of this study

The aim of the study was to develop a novel hydrogel 3D printed tablet loaded with MTX polymeric nanoparticles for oral drug delivery. To achieve this aim the following objectives are outlined:

1. To design a polymeric NPs using a TPGS functionalized polylactic-co-glycolic acid (PLGA) nano-framework loaded with MTX.
2. To undertake physicochemical characterization of the nanoparticle system by measuring particle size, morphology, chemical integrity and composition, drug loading efficiency and drug release.
3. To prototype and prepare a 3D printed oral tablet via additive manufacturing using 3D polymeric inks comprising a sodium alginate-gelatine (SA-GL) blended fixated with the MTX-loaded TPGS-functionalized PLGA NPs.
4. To complete thermal stability characterization of the SA-GL 3D printable ink employing thermogravimetric analysis.
5. To undertake *in vitro* pharmaceutical evaluation of the novel 3D printed oral drug delivery system fixated with the TPGS-functionalized PLGA NPs loaded with MTX.

1.4. Overview of the Dissertation

Chapter 1: serves as the introduction of the dissertation and describes various cancer treatment methods with specific focus on oral administration, applications, and advantages of using polymeric nanoparticles PLGA and TPGS, rational, motivation and aim of the study also discussed.

Chapter 2: provides a literature review of critical evaluation of oral 3D printed hydrogel/ nanocomposite tablet delivery systems for the treatment of cancer. It gives insight into the efflux mechanisms as barriers to intestinal absorption. It describes nanoparticles as the versatile and

beneficial platforms for targeted drug delivery whilst free MTX does not efficiently penetrate the plasma membrane barriers. It further emphasises that hydrogels inks incorporated with nanoparticles could be 3D printed for advancement of oral drug delivery.

Chapter 3: describes the development of Methotrexate-loaded TPGS-PLGA nanoparticle system. It includes the characterization of the PLGA-TPGS polymeric nanoparticles using FTIR, Zeta sizer and SEM microscope.

Chapter 4: is the optimization and validation of Envisiontec 3D Bioplotter using sodium alginate-gelatine hydrogel printable ink as a potential polymeric material for oral tablets.

Chapter 5: describes the 3D printing of oral drug delivery tablet using sodium alginate-gelatine printing ink incorporated methotrexate-loaded in polymeric blend of TPGS and PLGA nanoparticles. It includes the characterization of printed oral tablet using TGA and UV spectroscopy. Drug release profiles were also determined at buffer pH 1.2 and 7.4, simulating gastrointestinal environment.

Chapter 6: is a conclusion of research conducted, this includes limitations and recommendations of future work in designing and evaluating oral 3D printed chemotherapeutic delivery system.

CHAPTER 2
LITERATURE REVIEW
AN INCURSION INTO 3D PRINTED DRUG DELIVERY SYSTEMS AND NANOSYSTEMS FOR OPTIMAL CHEMOTHERAPY

2.1 Introduction

Cancer consist of a range of diseases that occur as a result of unregulated growth of malignant cells with potential to invade or develop to other organs. More than 9.6 million new estimated cases each year of cancer-related deaths are projected to increase in the near future with an estimation by the World Health Organization of ~13.1 million cancer-related deaths by the year 2030 (WHO, Global Health Observatory. Geneva: World Health Organization). Cancer is amongst the prevalent diseases that consistently give physicians, scientists and researchers new challenges. According to the WHO 2018, over the years cancer has been listed as one of the diseases that are to be treated with priority (WHO, Global Health Observatory. Geneva: World Health Organization). Conventional cancer treatments such as surgery, radiotherapy, and chemotherapy are highly regulated (Senapati, et al., 2018). Regulatory authority and organizations are responsible for the effective drug regulation required to ensure the safety, efficacy and quality of drugs, as well as the accuracy and appropriateness of the drug information available to medical professionals and the public. (Stones & Jewell, 2017)

Chemotherapeutic treatment has been reported to produce varying effects on patients and some patients may not respond well to such treatment. Additionally, most chemotherapeutic agents have non-specific targeting and fail to target the cancerous cells selectively without interacting with normal cells. Chemotherapy has been beneficial to some extent, however there are some drawbacks such as poor bioavailability, high-dose requirements, negative side effects, low therapeutic concentrations, development of multiple drug resistance, and non-specific targeting. The significance of improving drug delivery vehicles is to address these delivery-related challenges and deliver drugs to specific therapeutic action sites whilst minimizing unfavourable side effects (Senapati, 2018; Li, 2019). This carrier approach can deliver therapeutics either passively or actively to target cancerous cells and minimize adverse side effects whilst improving therapeutic efficacy.

The use of versatile materials, such as polymers, lipids, inorganic carriers, polymeric hydrogels, and bio-macromolecular scaffolds have resulted in enhanced bioavailability of chemotherapeutics

to tumour sites with elevated therapeutic efficacy (Singh, et al.,2019). Several chemotherapeutics are intricate and involve contribution of multiple combinational therapies (Bajetta, et al.,2007). Targeted therapies result in fewer adverse effects and are more effective in the treatment of cancer due to the possibility of using higher doses of drug. (Bahrami, et al., 2017). Nanoparticles is one of the most versatile and beneficial method of attaining drug targeting in drug delivery systems. Nanoparticles are defined as submicron colloidal particles in which the drug is absorbed, dissolved, or dispersed throughout the matrix and nano-capsules, in which the drug is confined to an aqueous or oily core surrounded by a shell-like wall (Maksimenko, et al., 2019).

Oral delivery strategies have gained interest for the treatment of a large variety of tumours such as colon, breast, gastric, ovarian, or lung cancer (Bajetta, et al., 2007). The limitations of mass-produced medicines are being addressed by new technologies being developed, whereby medicines can be made more personal (Alomari et al., 2015). Horst et al, 2018 showed some advantages, limitations, challenges, and perspectives pertaining to 3D printing of pharmaceutical grade formulations and polymers, used for drug delivery systems. This report discussed the possibilities to design and develop drug delivery devices by using different materials and techniques. 3D printing thus offers a unique solution to the limitations of mass-produced medicines (Horst).

This review thus aims to provide an insight in the advancement of nanocomposite hydrogels for nanomedicine. Recent advances in nanoparticle–hydrogel composites are presented with a focus on their synthesis, design, potential applications, and the inherent challenges accompanying these polymeric materials. 3D printing technologies are also reviewed as promising tools for preparing not only some of the conventional pharmaceutical dosage forms, but also nanogels used for oral chemotherapeutic delivery in biomedical and pharmaceutical applications.

2.2 Oral drug delivery

Oral drug delivery of chemotherapeutic agents offers many advantages to both patients and healthcare providers. There are however also challenges associated with the use of oral chemotherapeutic drugs (Sohail, et al., 2018). The effectiveness of the chemotherapeutic agents is highly dependent on their ability to cross cellular barriers to reach target sites as shown in Figure 2. 1. The lipophilic properties of chemotherapeutics play a major role on permeability across barriers in the absence of specialised transport systems, since these drugs may slowly diffuse through the plasma membrane barriers (Chana, et al., 2004). On the other hand,

hydrophilic and charged molecules may require specific transport mechanisms to facilitate cellular uptake and/or transcellular transport. However, the degree to which chemotherapeutics can accumulate within a tissue is normally limited due its tendency to permeate efflux pumps (Chana, et al., 2004). This review provides insight into the efflux mechanisms as barriers to intestinal absorption. The main site of absorption for ingested substances is small intestine. Chemotherapeutics are mainly absorbed by the gastrointestinal tract (GIT). The degradation and absorption of substances occurs from the intestinal lumen and intestinal enterocytes forming a selective barrier to xenobiotic. It has been reported that this barrier mainly depends on membrane transport systems and intracellular metabolising enzymes (Chana, et al., 2004). The magnitude of absorption of chemotherapies in the intestinal epithelium is a critical factor in determining the bioavailability of agents followed by plasma protein binding. The main challenge is that chemotherapies that penetrate through the apical membrane may be subjected to efflux transporters and extrude compounds back into the lumen (Walgren, et al., 2000).

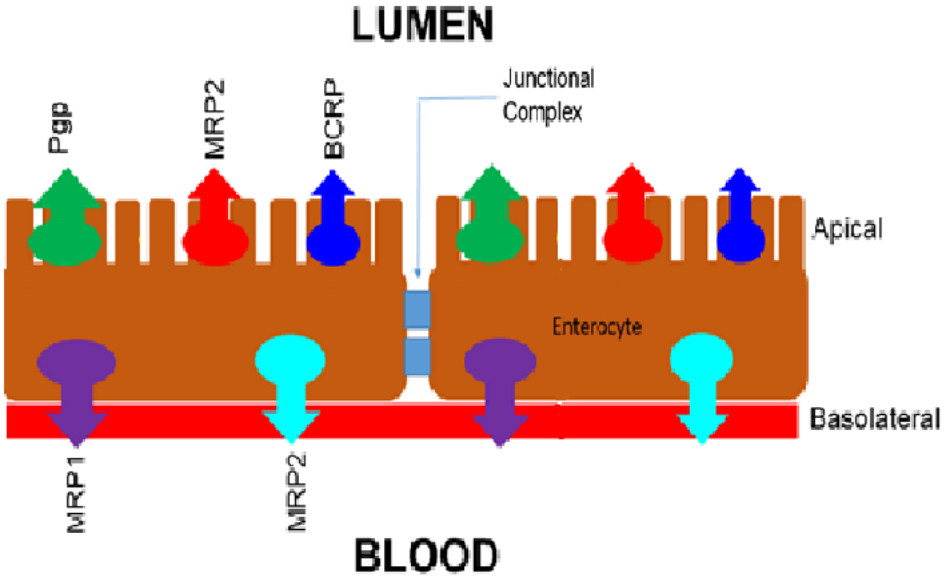


Figure 2. 1 Schematic overview of main drug transporters expressed on enterocytes in intestinal epithelia membrane: P-glycoprotein (Pgp); multidrug resistance-associated protein 1 (MRP1); multidrug resistance-associated protein 2 (MRP2); breast cancer resistance protein (BCRP) (Sohail, et al., 2018)

In this chapter, the summary of most important benefits associated with oral drug delivery is highlighted. This delivery route is convenient for patient and health care provider since it reduces the need for specialized expertise. The patient can normally self-administer oral medications. This

oral system improves patient compliance as there is no need for invasive needle related discomfort, special care or inconvenient time-consuming administration (Martínez-Martínez, et al., 2019). The oral delivery is a preference due vast area of intestinal high drug absorption. The varying physiological conditions in the intestinal system offers better chances of drug absorption compared to other types of drug delivery systems (Sohail, et al., 2018). Oral delivery systems are generally more cost-effective than other methods of drug administration. Oral delivery offers a reduced use of health care services since, there is limited need for specialized administration (Beloqui, et al., 2017). Oral delivery systems are capable of inducing pharmacodynamics that are superior compared to intravascular administration (Beloqui, et al., 2017). Sufficient plasma concentrations can be achieved thorough oral delivery for sustained inhibitory effect on cancer cells (Ruiz-Gatón, et al., 2018). This oral route can also be used in facilitating chronic treatments (Ruiz-Gatón, et al., 2018). Lastly, the oral drug administration is superior for controlled drug release compared to other methods of administration (Sardo, et al., 2019).

In this study the disadvantages in using oral chemotherapeutic drug delivery system are highlighted. The hepatic first-pass effect by the cytochrome P450 (CYP450) enzyme system extensively reduces the bioavailability of orally administered drugs (Shen, et al., 2019). Numerous cancer cells may overexpress the efflux protein P-glycoprotein (P-gp) which acts as the primary efflux pump for anti-cancer therapies. Cancer cells can develop overexpression of P-gp through genomic or non-genomic acquisition (Dyson, et al. 2019). Overcoming this source of drug resistance is of paramount importance as no effective multidrug resistance treatment has yet been developed due to the toxicity of P-gp blockers (Dyson, et al. 2019). The factors that determine the bioavailability of a drug after oral administration are the rate of dissolution in acidic gastric fluid and permeability across the enterocytes. Two elements that primarily influence these factors are physiochemical properties of the drug molecule and the actual physiological attributes of the gastrointestinal tract (Jiang, et al., 2019). Hydrophobic drugs are challenging to deliver orally and intravenously due to inherent inability to cross the cell membrane and reach the intracellular environment. This is due to the surrounding aqueous environment in tissues and organs (Aboul, et al., 2018). Poorly soluble drugs in oral dosage forms usually have variable and unreliable absorption leading to varying degrees of efficacy (Beloqui, et al., 2017). Therefore, there is an urgent need to develop new oral nanoformulation for targeted delivery with improved drug efficacy of cancer medication (Yang et al., 2015).

2.3 Methotrexate nanoparticles in cancer treatment

One of the significant challenges in cancer therapy is selective targeting of cancer cells. Targeted therapy provides solution to these challenges where small variances between cells can be used to differentiate between cancer- and normal cells (Mehata, Bharti and Singh). Targeted therapies present with fewer adverse effects and are more effective in cancer treatment due to the possibility of using higher doses of drug. (Bahrami, Hojjat-Farsangi and Mohammadi). Nanoparticles (NPs) are the most versatile and beneficial carriers for drug targeting in drug delivery systems. NPs are defined as submicron colloidal particles in which the drug is absorbed, dissolved, or dispersed throughout the matrix and nano-capsules, in which the drug is confined to an aqueous or oily core surrounded by a shell-like wall (Maksimenko, Malinovskaya and Shipulo). Benefits of nanoparticles additionally include specific tumour targeting, increased drug bioavailability and specific functionality (Amani et al., 2019). Using nanoparticles as drug carriers also has several further advantages which include increased stability, increased shelf life, and high carrier capacity (Haseeb, Khaliq and Yuk).

Methotrexate (MTX) is a folate antimetabolite which inhibits dihydrofolate reductase to block the synthesis of tumour cells resulting in the stunting of growth and reproduction of tumour cells (Zhang et al., 2014). MTX is used in the treatment of various types of malignancies, but high toxicity and short plasma half-life limits its use in current practice (Asfhari, Derakhshandeh, and Hosseinzadeh, 2014). MTX loaded poly (lactic-co-glycolic acid) (PLGA) nanoparticles show an increased antitumor activity due to the protection of PLGA from hydrolysis and decomposition as well as maintenance of the drug activity in a sustained release manner (Maleki et al., 2017). Wang et al (2013) theorized that the d-α-Tocopheryl polyethylene glycol 1000 succinate (TPGS) shows effective toxicity for cancer cells and thus could synergistically enhance the therapeutic efficacy of drug-loaded TPGS nanoparticles. Liang, et al. (2010) reviewed nanotechnology utilized to prevent tumour resistance in chemotherapy. They provided evidence that nanoparticles are an effective strategy for overcoming drug resistance in cancer cells. The reason for this is theorized due to cells internalizing nanomaterials below 100 nm. Hence, nanostructures have the ability to enter the cells due to nanoscale size (Kadari, Pooja and Gora).

Asfhari et al., (2014) fabricated MTX-loaded PLGA- poly (ethylene glycol) NPs by emulsification/solvent diffusion technique and observed the same pattern of initial burst release during the first hour of MTX release followed by sustained release. They also observed delayed release due to the diffusion of drug molecules through the polymeric matrix and its exit to the

dissolution medium. The results of the cytotoxicity evaluation conducted in this study demonstrated that NPs have a great effect on the cellular in vitro cytotoxicity and sustained-release character led to enhanced clinical antitumor effects.

MTX partially penetrate the blood-brain barrier, thus necessitate administration by high-risk intrathecal injections employed for the delivery to the tumours of the central nervous system (Malhotra and Prakash). The blood-brain barrier consists of capillary endothelial cells with primary function of protecting the central nervous system from harmful molecules and excludes most of small molecule drugs (>98%) and virtually all large molecule drugs (Masserini). Chemotherapy including MTX is the preferred anti-cancer treatment in brain tumours due to the possibility of severe injury during surgical intervention and radiotherapy (Li et al., 2018). Polymeric nanoparticles are widely employed as carriers for the transport of chemotherapeutic drugs across blood-brain barrier due to their smaller particle size, high structural integrity, ability to penetrate the tissues, ease of preparation, better biological fluids stability, flexible drug loading/release characteristics (Gao, 2008 and Jiang, 2006). However, nanoparticulate delivery systems have few limitations regarding their accuracy of tumour targeting and the ability to provide sustained drug release. Hence, a rational and strategic approach has focused on nanocomposite hydrogels with improved mechanical properties, response to different stimuli and sustained drug release Cho et al., 2018).

2.4 Nanocomposite hydrogels as 3D printable inks for advanced drug delivery

3D printing is an advanced manufacturing and rapid prototyping of 3D structures generated in a layer-by-layer manner through computer-aided design until the final artefact product is formed. 3D printing technology has crafted very complex structures that cannot be fabricated using traditional manufacturing methods such as the use of moulds (Chua, 2017; Lamichhane, 2019). 3D printing is an evolving technology with numerous applications in development of structures to systematically combat human diseases. Automated 3D bioprinters are a fairly new technology that provides high reproducibility and precise control of manufacturing structures (Shim et al., 2011). Hydrogel printable inks are formulated from natural biomaterial, and in special cases are combined to form a hybrid biomaterial (Groll et al., 2018). Hydrogel printable inks are well known materials used to produce robust artificial structures *via* 3D printing processes. Generating stable final architecture of the designed structure requires cross-linking hydrogel printing ink and this can be achieved during or immediately after printing (Groll, et al., 2018). Hydrogels are frequently used for fabrication of tissues or structures due to biocompatible materials and provide a highly

hydrated 3D environment for the cells (Groll, 2018; Zhu, 2011). Historically, natural hydrogels are commonly used for tissue engineering, including alginate, collagen, gelatin, and chitosan. In 3D printing, extrusion-based techniques using hydrogels for fabricating structures for drug delivery systems have been extensively studied (Amjadi, Hamishehkar and Ghorbani). Studies into several potential hydrogel formulations have shown that sodium alginate has great potential as a bio-ink. (Maher, Keatch and Donnelly). Bio-ink formulated with sodium alginate showed outstanding printing accuracy and printing precision. Divalent ionic cross-linkers are commonly used during or after the printing process to increase the strength and stability of printed structures to induce rapid gelation (Naghieh, Karamooz-Ravari and Sarker). Several other methods have also been employed and shown to be effective in controlling the gelation and solidification of printed structures comprised of hydrogels (Li, Tan and Leong). Variations of concentrations, viscosity, and the temperature of the printing bio-ink and the printing platform can control the rate of the bio-ink gelation (Jin, Lui and Chai). Hydrogels have a diverse tuneable feature that can be customized for specific therapeutics (Qiu, et al., 2001). Crosslinked hydrogel networks can protect drugs from harmful environments, such as enzymes and low pH in the stomach (Sharpe, et al., 2014). Hydrogel from alginate are favourable biomaterial since they are naturally occurring, biodegradable, non-toxic, and non-immunogenic linear polysaccharide composed of guluronic and mannuronic acids (Lee, et al., 2012). Alginate is a highly biocompatible low-cost marine material that is obtained from the cell walls of brown algae (Oyen, et al., 2016). This has encouraged researchers to use alginate as a one of components in the designing and fabrication of hydrogel printable inks (Oyen, et al., 2016). Alginate is composed of (1–4) linked β-D-mannuronic and α-L-guluronic acids (Szekalska, et al., 2016). Furthermore, alginate biomaterial is favourable to researchers since it is a polysaccharide that is negatively charged, and it is known that generally positively charged materials provoke an inflammatory response. Alginate is also a soluble biopolymer that supports cell growth and exhibits high biocompatibility and has an ability to trap hydrophilic and other molecules by capillary forces in an alginate matrix and these molecules are still able to diffuse (Kulseng, Skjåk-Braek and Ryan). These feature makes alginate hydrogels ideal for hydrogel printable ink formulations (Oyen et al., 2016).

2.5 3D Printing: State-of-the Art in Drug Delivery Systems Design

In the past few years, it has been realized that the effective optimization of chemotherapeutics is required with advancements in drug delivery strategies involving nanotechnological platforms (Jayanta Kumar Patra). A drug delivery system is the carrier through which active pharmaceutical

ingredients are effectively distributed throughout the body to the specific site of infection. There are several different drug delivery systems designed for specific pharmaceutical goals such as targeted-release, extended release, and combination-release systems (Gaurav Tiwari). The limitations of mass-produced medicines are addressed by new technologies being developed with therapeutics prepared to be more personal (Alomari et al., 2015). Horst et al, 2018 showed some advantages, limitations, challenges, and perspectives pertaining to 3D printing of pharmaceutical grade formulations and polymers, used for drug delivery systems. This report discussed the possibilities to design and develop drug delivery devices by using different materials and techniques. 3D printing was reported to offer a unique solution to the limitations of mass-produced medicines (Horst). 3D printing brings a new dimension to drug delivery system, making it possible to not only have specific release strategies, but also patient specific doses and alterations. 3D printing opens up a host of advantages and opportunities in personalised pharmaceutical treatments (Horst). This printing strategy allows exact quantities of a medicine to be printed based on the initial printing ink drug concentration and the actual measurements of the printed tablet. Physically adjustments of the tablet dimensions or infill percentage can easily alter individual printed doses. The power of pioneering technologies such as 3D printing can be used to support manufacturing practices and could revolutionise the design of medicines for individual patients (Trenfield, Awad and Goyanes). Dosing requirements in paediatric and geriatric patients can be significantly different to normal patient doses due to changes in pharmacokinetics, which is a challenge when medicines are manufactured at a specific strength or formulation type. Often, the medications are then split or crushed to obtain the required dose, which could lead to incorrect dosing or dose dumping. Dispensing of individualised doses medicine on-demand can increase access to medicines and reduce excess and wastage (Trenfield, Awad and Goyanes). In a study conducted by Beck et al. (2017) first attempt was made to conjugate nanotechnology and 3D printing. In this study, polymeric nanocapsules were successfully loaded in fused deposition modelling (FDM) printed devices, prepared from printable polymeric filaments (Trenfield, Awad and Goyanes).

This review thus aims to provide an insight in the advancement of nanocomposite hydrogels for nanomedicine. Recent advances in nanoparticle–hydrogel composites are presented with a particular focus on their synthesis, design, potential applications, and the inherent challenges accompanying these polymeric materials. 3D printing technologies are also reviewed as promising tools for preparing not only some of the conventional pharmaceutical dosage forms,

but also nanogels used for oral chemotherapeutic delivery in biomedical and pharmaceutical applications.

3D printing offers several advantages in the manufacturing of solid oral dosage forms. Firstly, fast prototyping and optimisation of different parameters provides the opportunity to enhance and optimise the dosage form in vastly reduced timelines when compared to conventional manufacturing. Due to its effortless adaptability, 3D printing overcomes a great challenge in manufacturing of variations in dosage strength which can increase bioavailability. Oral delivery devices can also be customised to the patient, incorporating different medications and reducing the need to take multiple tablets. The flexibility of 3D printing also increases its ability to be adaptable to targeted delivery and release profiles. (Lim, Kathuria and Tan)

2.5.1 Methods of 3D Printing

The following 3D printing techniques were developed including selective laser sintering (SLS), inkjet powder-bed 3D printing and fused deposition Modelling (FDM) (Ozkan, Ienina and Barakh Ali). SLS manufactures detailed structures by use of a laser beam that selectively sinters powder particles. SLS is especially useful in the production of alterable release profiles of dosages. Another advantage is that any un-sintered powder can be reused thereby minimising waste (Fina, Gonyanes and Madla). Inkjet powder-bed 3D printing uses an ink-jet head that jet-dispenses a liquid binder solution onto a flattened powder bed resulting in particles of the powder carrier to adhere to each other and form the printed object (Shi, Tan and Nokhodchi). 3D inkjet powder-bed printing enables accurate deposition of the printing ink at a substantial scale. This makes it an excellent choice for manufacturing high volumes of drug delivery devices whilst still providing the choice of flexible and personalized manufacture (Clark, et al. 2017). FDM uses a nozzle to print a Computer-aided design 3D pattern layer by layer (Long, Gholizadeh and Lu). FDM 3D printing has been employed effectively in the production of delayed release printlets without the need for an outer enteric coating. FDM can also modify release profiles of dosages tailored to a specific patient's needs (Goyanes, et al., 2017; Fina, et al. 2017). 3D-Bioplotters have been developed specifically for the printing of hydrogels for use in the biomedical industry. These printers consist of a syringe and a stage for controlling the ejection position of the solution. These printers can create custom-designed 3D structures from biocompatible hydrogels. (Taira, Ino and Robert).

2.5.2 Limitations of 3D Printing in Chemotherapeutic Drug Delivery

The application of 3D printing in pharmaceutics can provide many benefits, however there are still several limitations that have prevented the mainstream approval of 3D printing in drug delivery (Bakarich, Gorkin III and in het Panhuis). Due to the nature of 3D Printing, there are still limited materials that can be used as raw materials for 3D printers (Tariq and Mazhar). These materials are limited by factors such as biocompatibility, heat-sensitivity, degradation and printability. (Aquino, Barile and Grasso). The final product produced by 3D printing also generally lacks the accuracy needed in commercial manufacturing. This enhances the requirement of additional production steps such as grinding or polishing. (Solanki, Tahsin and Shah). Regulatory approval and product patenting are another concern. The possibility of 3D printing pharmaceutical counterfeits is significant due to its availability and the ability of regulatory agencies and pharmaceutical companies to control this is limited. An estimated 5% of medicines are counterfeit, leading to huge financial losses for the pharmaceutical industry. More importantly though, counterfeit products have been found to be low quality and may lead to a great health risk to public health. (Stones and Jewell).

2.6 Concluding Remarks

Cancer is a prevalent disease that has driven scientist to discover alternative advanced drug delivery systems. Through research it has been established that oral drug delivery reduces the need for specialized expertise. The patient can normally self-administer oral medications. This oral delivery route has its own share of limitations including, the metabolism of chemotherapeutics by the cytochrome P450 enzyme system which extensively reduces the bioavailability of orally administered chemotherapeutics. The quantities of chemotherapeutic absorption within the gastrointestinal (GIT) tract is limited by efflux transporters. Several chemotherapeutics lacks lipophilicity and are unstable at harsh GIT pH environment. This present study highlighted that chemotherapies such as MTX are responsible for stunting of growth and reproduction of cancer cells since they undergo quick metabolism by enzyme CYP450 with reduction in bioavailability and interaction with the protein P-glycoprotein (P-gp). Furthermore, the use of nanoformulation as drug delivery system may control the drug release and enhance the distribution of nanoformulated chemotherapies to targeted sites. However, nanoparticulate delivery systems have few limitations regarding accuracy of tumour targeting and the ability to provide sustained drug release. Hence, a rational and strategic approach has focused on nanocomposite hydrogels with improved mechanical properties, response to different stimuli and sustained drug release.

This chapter provided a concise incursion into the use of 3DP for the design of drug delivery systems and outlined the potential of 3DP to achieve more precise anti-cancer drug delivery by merging with nanotechnology. Previous research had demonstrated that there are many benefits to using nanoparticles to control drug release across biological membranes with 3DP offering an added advantage of customizing oral doses. In particular earlier research has suggested that combining the targeting abilities of NPs with the dosing flexibility of 3DP can overcome several challenges to optimize oral delivery of anti-cancer drug molecules.

CHAPTER 3
PHASE 1: SYNTHESIS OF METHOTREXATE-LOADED TOCOPHERYL POLYETHYLENE GLYCOL SUCCINATE-FUNCTIONALIZED POLYLACTIDE-CO-GLYCOLIC ACID NANOPARTICLES

3.1 Introduction

Nanoparticles (NPs) have been proven beneficial to obtaining superior tumour targeting and increasing drug bioavailability via surface functionalization (Amani et al., 2019). Numerous cancer cells genomically or non-genomically acquire overexpressed P-gp that's acts as the primary efflux pump for anti-cancer drug molecules. P-gp overexpression and P‑gp-mediated efflux leads to anti-cancer drug resistance and to date there is no effective multi-drug resistance treatment that has been developed due to the toxicity of P-gp blockers (Ghandi and Roy).

d-α-tocopheryl polyethylene glycol 1000 succinate is derived from vitamin E and consists of amphiphilic chains. TPGS is specifically used to overcome the efflux protein P-glycoprotein (P-gp) at a concentration that is below the critical micelle concentration through inhibition of ATPase (Robert W. Robey). TPGS has been proven to be a safe and unlikely cause of adverse pharmacological reactions or drug interactions (Conglian Yang). The head of TPGS is non-ionic and lipophilic while the tail is hydrophilic polyethylene glycol (PEG). Therefore, TPGS also be used as a nonpolar surface-active agent in nanoparticulate drug delivery systems to carry both hydrophobic and hydrophilic medications. (Dyson, et al. 2019; Tan, et al. 2017; Collnot, et al. 2006).

Poly (lactic-co-glycolic acid) (PLGA) is a biocompatible synthetic co-polymer consisting of Polyglycolide (PGA) and Polylactic acid (PLA). PLGA nanoparticles show an increase antitumor activity and maintenance of the drug activity in in a sustained release manner due to the protection provided by PLGA from hydrolysis and decomposition (Rezvantalab, et al. 2018; Maleki et al., 2017). Hence, biodegradable PLGA has shown enormous potential as a drug delivery carrier for targeted cancer treatment (Siegel, The Poly Lactic-co-Glycolic Acid (PLGA) as Biodegradable). Polymeric PLGA has been approved by Food and Drug Administration (FDA) for therapeutic nanoformulation preparation (Makadia, 2011). These PLGA copolymers are robust, biodegradable and highly biocompatible and have been extensively studied as delivery vehicles

for drugs, proteins and various other macromolecules such as deoxyribonucleic acid, ribonucleic acid and peptides (Siegel, 2011). It has been reported that PLGA is able to deliver its load within proper duration with improved bio-distribution and drug efficacy for intended therapeutic effect (Siegel, 2011) (Yang YY1). Research conducted by Murugushe (2015), investigated the physiochemical properties, controlled release characteristics, stability and cellular uptake of chitosan-PGLA and PLGA nanoparticles loaded with α-tocopherol for gastrointestinal tract delivery (Murugeshu et al., 2011). *In vitro* and *ex vivo* results showed that PLGA and Chitosan-PLGA nanoparticles were efficiently taken up by the gastrointestinal tract with improved bioavailability of α-tocopherol (Murugeshu, et al., 2011). A study conducted by Lucia (2019), investigating the fate PLGA nanoformulation for local delivery of therapeutic drugs in gastro intestinal tract after oral administration. Through *ex vivo* analysis it was established that PLGA nanoformulations were detected in gastrointestinal tract for up to 24 hours (Lucia).

3.2 Methods and Materials

3.2.1 Materials

D-α-Tocopherol polyethylene glycol 1000 succinate (TPGS1000), Poly (D,L-lactide-co-glycolide)(PLGA), Methotrexate (MTX), distilled water, HPLC grade acetone, ethanol and acetonitrile, mannitol were purchased from Sigma (Sigma-Aldrich, Missouri, USA). Simulated gastrointestinal environment (at buffer pH 1.2 and 6.8) was prepared from analytical grade reagents according to the method reported by (Sardo, et al., 2019). All of the reagents procured were of highest analytical grade.

3.2.2 Preparation of Methotrexate-loaded TPGS-PLGA nanoparticulate system

The MTX-loaded TPGS-functionalized PLGA NPs were prepared using a modified nanoprecipitation technique adapted from Cerqueira and co-workers (2017). Briefly, 200 mL of deionized water was mixed with ethanol (80 mL) to prepare a 40%w/v ethanol-aqueous solution. TPGS (2 mL) was then dissolved in 100 mL of the ethanol-aqueous solution using continuous magnetic stirring at 90 °C for 2 hours until TPGS was completely dissolved. Thereafter 50 mg of MTX was dissolved in 100mL of the TPGS solution using a magnetic stirrer set at 30 °C for 20 minutes.

Separately, a PLGA acetonitrile mixture was prepared by dissolving PLGA (700 mg) in acetonitrile (100 mL). The PLGA solution was then added dropwise (1 mL/min) in a volume ratio of 1:10 to the TPGS solution under gentle magnetic stirring for 20 min at 35˚C to allow self-assembly of the

NPs. The excess organic solvent was removed by evaporation using a heated magnetic stirrer set at 80 °C for 2 hours under a fume hood. The nanoparticles solution was then filtered thrice using a 0.45 µm Millipore syringe filter and immediately lyophilised and stored at 2 ˚C.

3.2.3 Componential analysis of chemical structure integrity post nanoparticle formation

In order to assess the chemical integrity of native and combined components of the MTX-loaded TPGS-functionalized PLGA NPs, Fourier-Transform Infra-Red (FTIR) spectroscopy was used to identify and characterise the pharmaceutical stability of the MTX, TPGS and PLGA in their native and combined state (Lawson, Ogwu and Tanna). The analysis was set up to also determine what was the chemical stability impact of loading MTX in the PLGA NPs and if there were any functionally significant changes to be observed. The FTIR spectra was recorded at 20°C ranging from 500-4000cm^{-1} for samples of MTX, PLGA and the MTX-loaded TPGS-functionalized PLGA NPs.

3.2.4 Nanomiretic characterization of the MTX-loaded TPGS-functionalized PLGA nanoparticles

Nanomiretic characterization was undertaken to determine the surface morphology, particle shape, size, density, and surface energy using various techniques. A Zetasizer NanoZS (Malvern Instruments Ltd, Malvern, Worcestershire, UK) was used to determine the particle size and zeta potential of the NPs. The NPs were suitably dispersed in deionised water, filtered (0.22µm filter Millipore Co., MA, USA) and placed into disposal cuvettes (for size measurement) or capillary cells (for zeta potential determination). The viscosity and refractive index of the continuous phase were set to those specific to de-ionized water. Measurements were taken in triplicate (N=3) for each sample to obtain a size distribution and zeta potential profile.

3.2.5 SEM Characterisation of MXT-loaded TPGS-PLGA nanoparticles

The nanoparticle morphology was examined using Scanning Electron Microscopy (SEM). Powdered samples of the nanoparticles were placed onto an aluminium specimen stub covered with a double-sided carbon adhesive disc and sputter-coated with both palladium and gold for 4 min at 20 KV. SEM images of the Methotrexate-loaded TPGS-PLGA nanoparticles samples were viewed using a SEM (SIGMA VP, Zeiss Electron Microscopy, Carl Zeiss Microscopy Ltd; Cambridge, UK).

3.2.6 Thermal analysis Methotrexate-loaded TPGS and PLGA nanoparticles.

To characterize the thermal behavior of Methotrexate-loaded TPGS-PLGA nanoparticulate, TGA and DSC were performed using TGA (PerkinElmer STA 6000, Beaconsfield, United Kingdom) and a Mettler Toledo, DSC1, STARe Instrument (Schwerzenback, Switzerland) respectively. The analysis was performed for each reactant, drug and unloaded nano-formulation sample. For TGA, 5-10 mg sample was carefully weighed and placed in a crucible. Prior to analysis, standard temperature mode was selected, and samples were tested in the range of 30–900 °C with a 10 °C/min temperature rise and 20 ml/min rate of nitrogen purging. For DSC, 5-10 mg of each sample was carefully weighed and sealed in an aluminum crucible. Standard temperature mode was selected, the baseline was optimized, and each sample was tested in the -10–300 °C with a 10 °C/min temperature rise and 20 ml/min rate of nitrogen purging.

3.2.7 *In vitro* evaluation of Methotrexate release from the TPGS-PLGA nanoparticles.

To investigate the *in vitro* release of MXT from the TPGS-PLGA nanoparticles, Methotrexate-loaded TPGS and PLGA nanoparticles (N=3) was incubated in 30 mL of PBS and positioned in an orbital shaking incubator at 37 °C for 24 h. Release of MXT was determined at different pH conditions 1.2 and 7.4 to mimic the stomach pH and intestinal pH. Sampling occurred at specified time interval (5, 30, 60, 90, 120, 180, 240, 300, 360, 420,480 and 720 minutes), however for stomach release simulation was conducted up to 120 minutes. 1 mL samples were collected as per time intervals, fresh buffer solution was added to maintain sink condition. Samples were centrifuged at 5000 rpm for 10 min to allow nanoparticles settled into pellets. Supernatants were then analysed for UV absorption of MXT at 303 nm using the Nanophotometer UV/Vis spectrophotometer NP80 (Implen, München, Germany).

3.3 Results and Discussion

3.3.1 Assessment of MTX-loaded TPGS-functionalized PLGA nanoparticles

The nanoprecipitation method used in this study to synthesise the MTX-loaded TPGS-functionalized NPs nanoparticles produced stable nano-constructs with desirable yields and unimodal particle distribution. The nanoparticle solution was collected as a white free-flowing powder post lyophilization. Upon storage at 2 °C the nanoparticle powder bed was easily reconstituted for further nanomiretics characterization.

3.3.1.1 Assessment of nanoparticle size and zeta potential

The results of the nanoparticle formulation size distribution and zeta potential investigations in the current study showed a mean nanoparticle size of 186.9 nm and a small particle size distribution with a PDI of 0.157 in demonstrated Figure 3.1. The particle size of the nanoparticle formulations was established to be within the effective therapeutic range for the treatment of cancer.

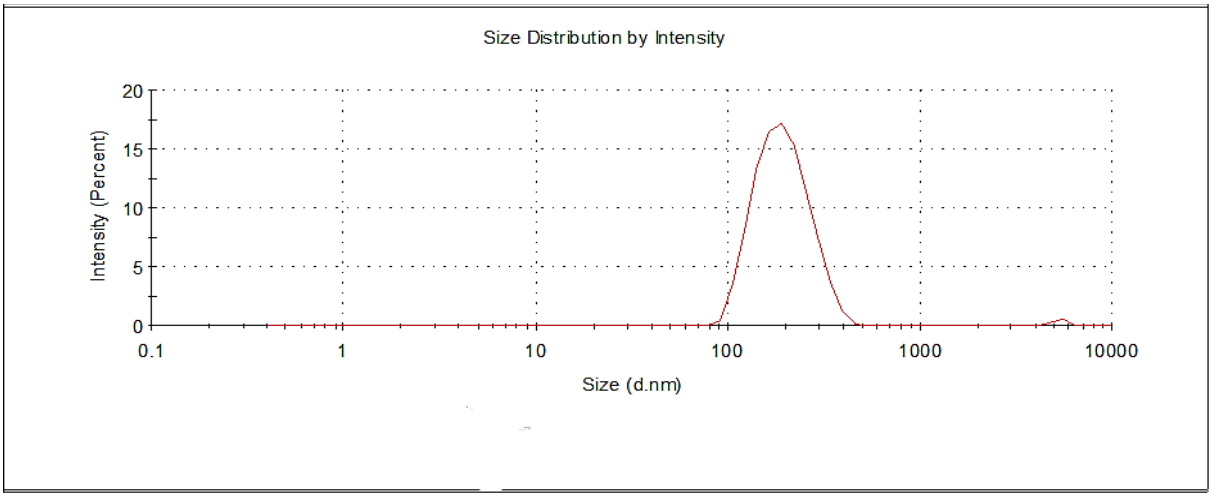


Figure 3. 1 Particle size distribution profile of Methotrexate-loaded polymeric TPGS-PLGA nanoparticles (nanoparticle formulation).

Nakumara (2017), stated that characterization of nanoparticles is important in order to correlate physicochemical properties of nanoparticles with biological responses and ensure that results are reproducible and meaningful (Nakumara, et al., 2017). Nanoparticles have highly tuneable size, structure, and surface properties. Nanoparticles are at a nanometre scale and exploited as carrier platforms for chemotherapeutics deliveries across membrane barriers (Nakumara, et al., 2017). Shahed (2018) reported that the nanoparticles size has an important role in cellular uptake. The cell membrane permeability to nanoparticles is largely determined by the nanoparticle size and surface composition. A crucial step in chemotherapeutic cellular uptake is the physical interaction between the nanoparticles and the cell membrane which may results in clustering of nanoparticle on the cell surface and consequently penetrate through the plasma membrane (Behzadi, 2018; Salatin, 2017). Numerous hypothetical models have been proposed to evaluate the lower-threshold radius of nanoparticles to be endocytosed (Zhao, et al., 2018). Several research studies presented a two-step model, which incorporates cells and ligand-coated spherical nanoparticle in thermodynamic equilibrium. It was expressed that nanoparticles formulations with minimum radius is required to undergo endocytosis process. The minimum radius required is based on the

energy released from ligand-receptor adhesion strength and the energy needed for bending the membrane (Behzadi, et al., 2018). Furthermore, several studies have conducted analysis on electrostatic interactions between nanoparticles and the cell membrane to understand the endocytosis of nanoparticles. The results showed that nanoparticles clusters have higher rates of internalization than single nanoparticles (Behzadi, 2018; Zhang, 2015). Nanoparticle size has significant influence on the ability to effectively reach the target site. Nanoparticles generally should to be less than 150 nm to traverse the endothelial barrier, however in cancer cells optimum nanoparticle size has been found to be between 70 and 200 nm (Gaumet, Vargas and Gurny). Narrow size distribution in nanoparticles are a key component in assuring the regulation of drug release rate, bioavailability and drug solubility (Beck, et al., 2017).

The zeta potential measured for the nanoparticle formulations in the current study was -31.4 mV as seen in Figure 3.2. The higher surface charge of the nanoparticle formulations improved stability and reduced the risk of excessive aggregation and poor distribution.

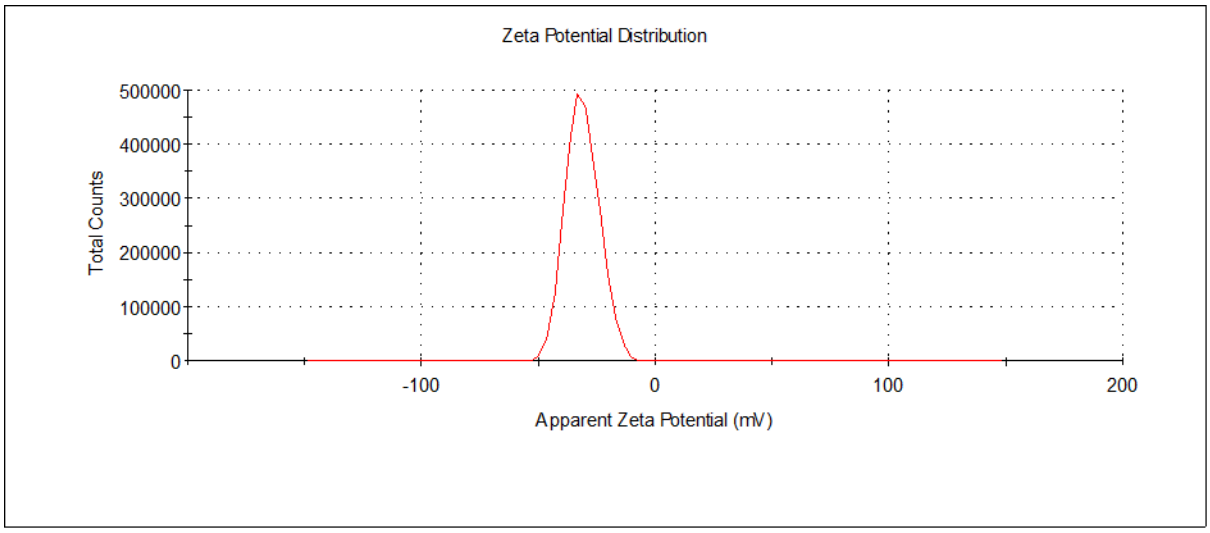


Figure 3. 2 Distribution profile of Zeta Potential of the Methotrexate-loaded TPGS-PLGA nanoparticles (nanoparticle formulation).

Positively charged nanoparticles have electrostatic interactions with the cell membrane's negatively charged phospholipid elements which increases absorption of circulating proteins. Nanoparticles coated with proteins are easily targeted and eliminated by macrophages. The increased clearance of the nanoparticles by the macrophages has a direct influence on the

effectiveness of the therapeutics. Higher surface charge of particles prevents the aggregation of nanoparticles due to the increase in repellent energy. Zeta Potential values of above 30mV has been proven to provide good stability of the nanoparticles in suspension with reduced aggregation and good dispersion.

3.3.1.2 Assessment of nanoparticle morphology

The polydispersity index (PDI) and zeta potential parameters were analysed, and it was determined that the sample and molecule distribution was uniform. Collectively, PDI were less than 0.2. The nanoparticles fabricated were collectively less than 200 nm. The zeta potential values collectively were -31.4 mV in average. The image in Figure 3.3 was captured by the scanning electron microscope (SEM) and the nanoparticle formulations were well distributed with spherical morphologies that had a size between 91nm and 200 nm. The particle size established in the SEM were considerably aligned to those established in the results from the Zeta Particle Size Analysis.

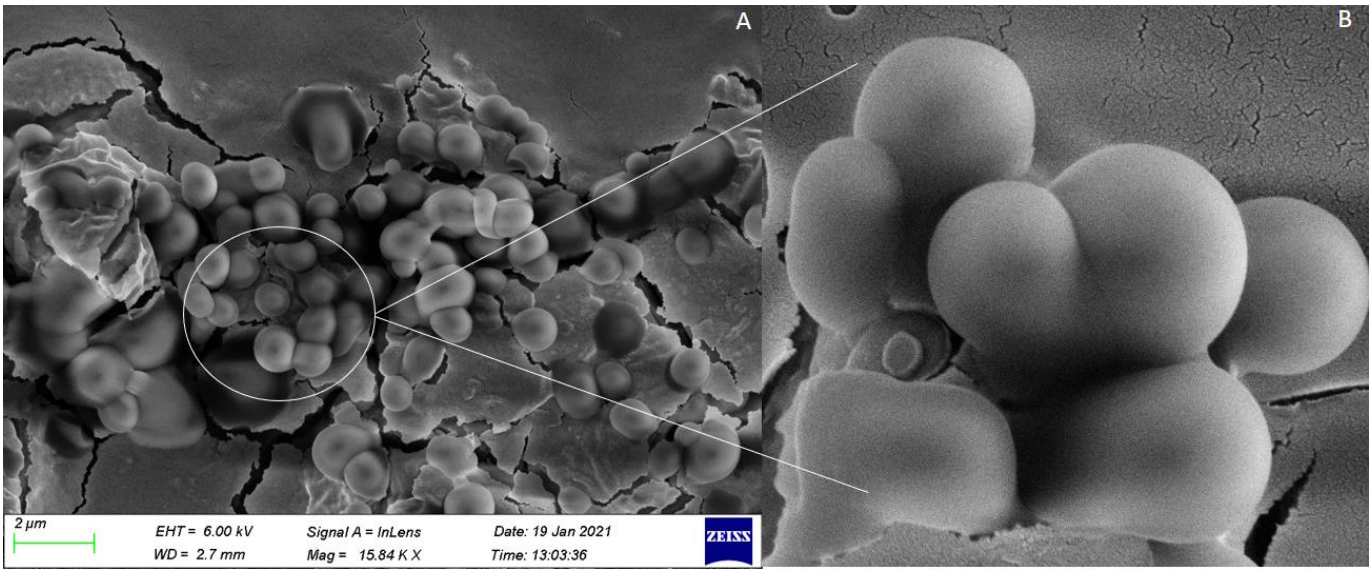


Figure 3. 3 Gold-platinum sputtered SEM Micrograph of Methotrexate-loaded TPGS-PLGA nanoparticles. (A) Magnification = 15.84 KX; Voltage =6.00 kV (B) Magnification = 44.34 KX; Voltage =6.00 kV. SEM of optimized Methotrexate loaded nanoparticle formulation showing sphericity, smooth surface of nanoparticles.

3.3.2 Assessment of MTX-loaded TPGS-functionalized PLGA nanoparticles thermal stability

3.3.2.1 Thermogravimetric analysis of MTX-loaded TPGS-functionalized PLGA nanoparticles

The TGA thermogram of unloaded TPGS-PLGA nanoparticles displayed decomposition pattern as shown in Figure 3.4. Initially, 30% weight was lost up to 350 ◦C, followed by a rapid decomposition at 430 ◦C, approximately 98% weight lost. Similarly, MXT-loaded TPGS-PLGA nanoparticles also exhibited two-stage weight loss. Initially, less than 30% weight was lost up to 350 ◦C, followed by a rapid decomposition with a weight loss of approximately 95% from a temperature of approximately 360 ◦C to 440 ◦C. The TGA of MXT showed moderately different thermogram where there was a slight decomposition from 40 ◦C to 200 ◦C, approximately 15 % weight lost. Followed by a rapid decomposition from approximately 210 ◦C to 250 ◦C, approximately 40% weight lost, and the final decomposition took place from approximately 300 ◦C, approximately 90% weight lost. This is also confirmed by TGA thermogram reported by Dixit et al., 2014.

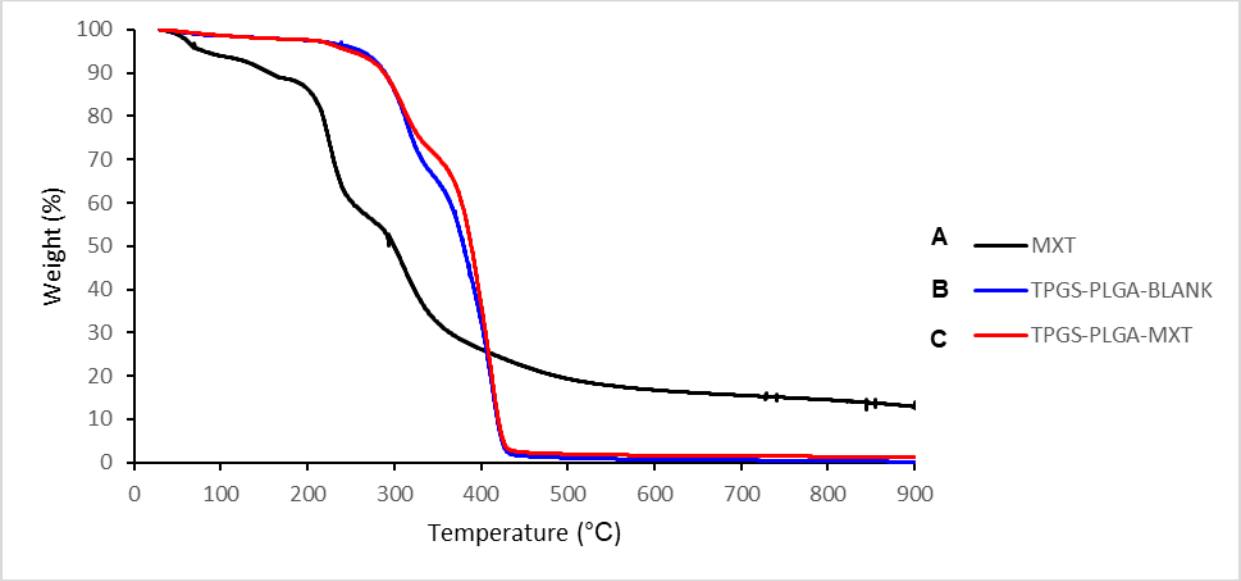


Figure 3. 4 (A) TGA curves of methotrexate (MXT). (B) TGA curves of blank PLGA nanoparticles. (C) TGA curves of the Methotrexate-loaded in polymeric TPGS-PLGA nanoparticle.

3.3.2.2 Differential scanning calorimetry analysis of MTX-loaded TPGS-functionalized PLGA nanoparticles

Heat flow curves (DSC curves) depicted in Figure 3.5 for thermal characterisation of Methotrexate-loaded in polymeric TPGS-PLGA nanoparticles showed big endothermic peaks. Identifiable differences in melting temperatures of transitions were obtained. DSC thermogram of TPGS-PLGA nanoparticles (Blank) showed a sharp endothermic peak, the melting point at temperature between 30-40 °C as shown in Figure 3.5, this maybe be due to low melting point of TPGS. MXT-loaded in polymeric TPGS-PLGA nanoparticles also showed a sharp endothermic peak at 30-40 °C, the MXT melting temperature peak was noted, broad endothermic peaks were visible at 130-160 and 190-230 °C, this is also confirmed by DSC thermogram reported by Pereira et al, 2013

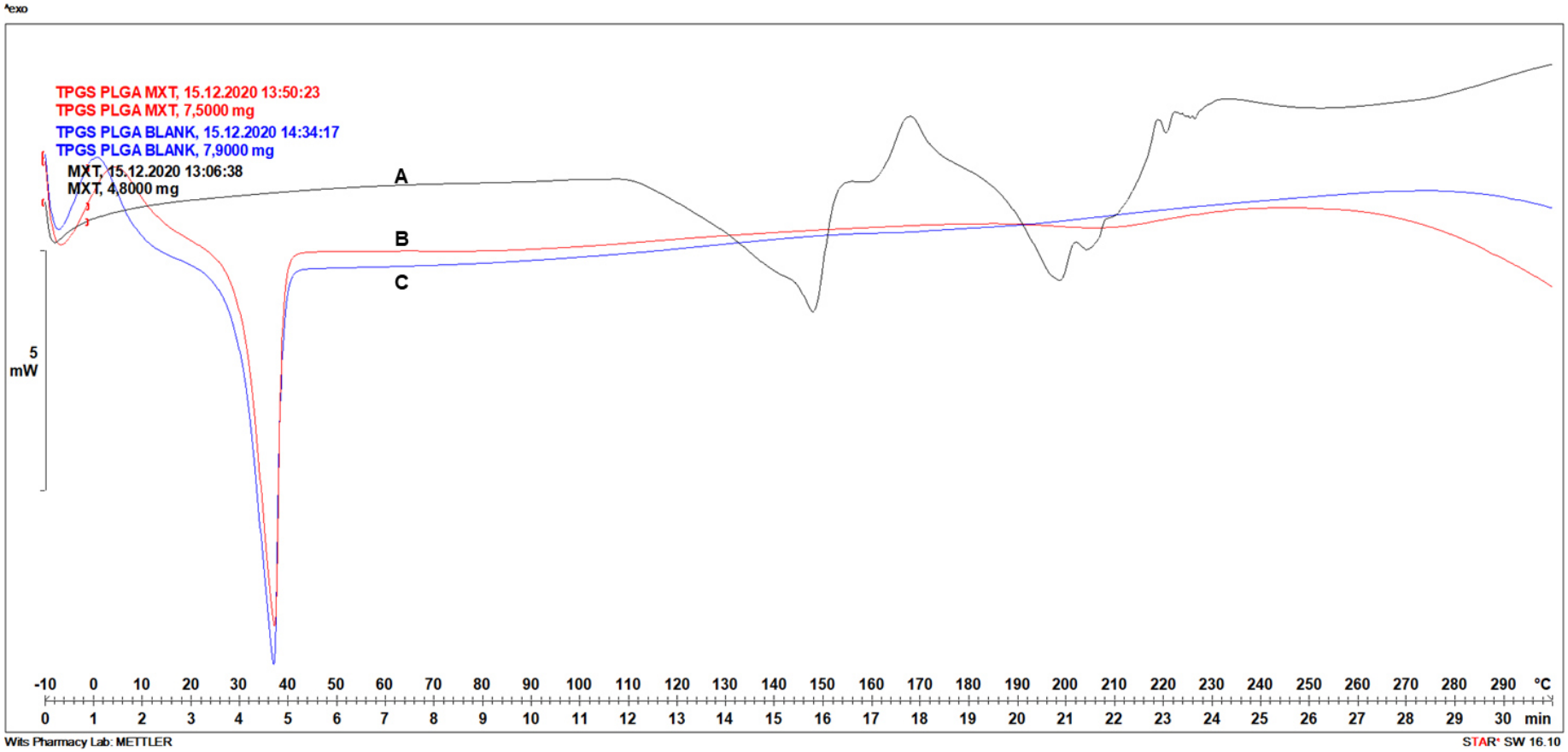


Figure 3. 5 (A) DSC curves of methotrexate (MXT). (B) DSC curves of blank PLGA nanoparticles. (C) DSC curves of the Methotrexate-loaded in polymeric TPGS-PLGA nanoparticle.

3.3.3 Evaluation of the chemical stability and integrity of the various nanosystem components

The FTIR spectra of PLGA, MTX and the MTX-loaded TPGS-functionalized PLGA NPs are shown in Figure 3.6. MTX showed typical waning of the broad signal from 3500-3000 cm^{-1} and sharpening of signals corresponding to O–H stretching from carboxyl groups and N–H stretching. Peaks at 1600-1670cm^{-1} linked to C=O stretching (–C=O stretching from carboxylic group and C=O stretching from amidic group) and 1400-1200 cm^{-1} corresponded to –C–O stretching from carboxylic group which are associated with -OH, C=C and C-O functional groups of MTX (Figure 3.6a). All the bands identified in the FTIR spectrum are in accordance with the molecular structure of MTX (Fulias, Popoiu and Vlase). The FTIR spectrum of PLGA-TPGS exhibited absorption peaks between 1000 and 1260cm^{-1} related to C–O single bond extensions and the broad absorption band at 2700 and 3000cm^{-1} assigned to O–H stretching and implies the existence of free hydroxyl groups of PLGA (Figure 3.6b). The carbonyl band of TPGS appears at 1,739 cm^{-1}. The peaks seen at 1650-1100cm^{-1} are attributed to the stretching vibrations of O–H as also shown by (Simsek, Eroglu and Kurum). The FTIR spectrum of the MTX-loaded TPGS-functionalized PLGA NPs displayed harmonious peaks to PLGA and MTX (Figure 3.6c) with the NPs imbibing similar chemical composition suggesting no significant chemical interaction between the functional groups of MTX and PLGA during formation of the NPs This is supported by similar studies in the literature (Maleki, et al., 2017)

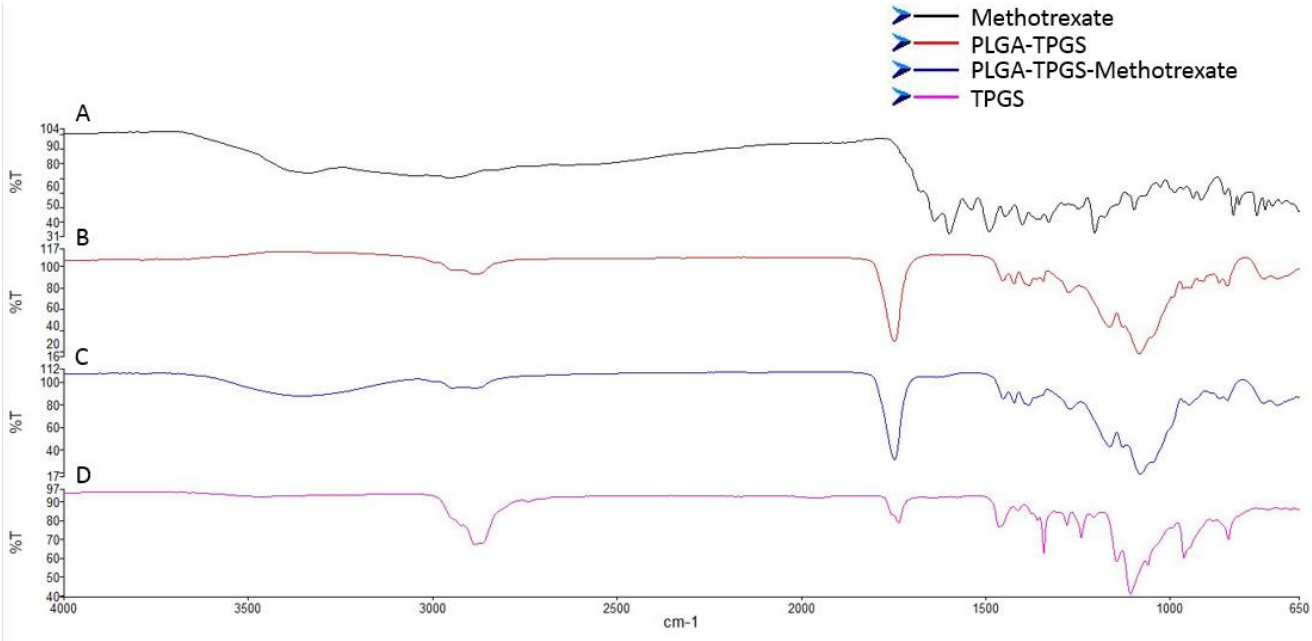


Figure 3. 6 (A) FTIR spectra of methotrexate (MXT). (B) FTIR spectra of PLGA-TPGS. (C) FTIR spectra of Methotrexate-loaded in polymeric TPGS-PLGA nanoparticles (nanoparticle formulation). (D) FTIR spectra of TPGS.

3.3.4 Drug Release Kinetics of Methotrexate from TPGS and PLGA nanoparticles

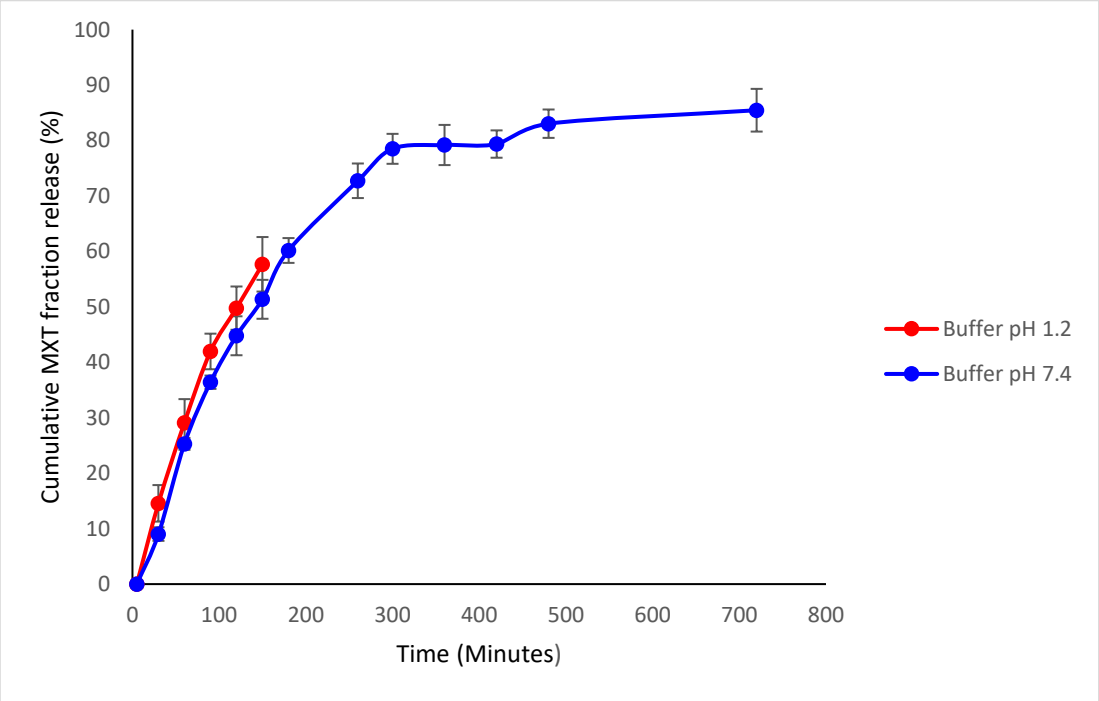


Figure 3. 7 *In vitro* release of MXT from TPGS-PLGA nanoparticles at a stomach acidity of pH 1.2 and intestinal environment of pH 7.4 (n=3, mean ± SD)

MXT release from the TPGS-PLGA nanoparticles occurred in two phases with an initial uniform rapid release of up to 80% within 5 hours followed by a slow continuous cumulative fractional release phase over 24 h across the pH media of 7.4. The gastric (pH 1.2) simulation was simulated for up to 2.5 hours because the administered content would have passed through the stomach at around this time. The MXT release pattern observed from the TPGS-PLGA nanoparticles indicated that the formulation is suitable for oral dosing and there were no significant MXT release differences between pH 1.2 and 7.4 up to 2.5 hours. The MXT was released up to 85 in 24 hours in an intestinal simulated environment of pH 7.4

3.4 Concluding Remarks

In Phase 1 of this study, the PLGA-TPGS polymeric nanoparticles were synthesized and characterized using FTIR. The FTIR displayed comparable peaks to the PLGA and MTX, showed that the nanoparticle formulations have similar chemical composition and suggesting

that there was no significant chemical interaction between the functional groups of MTX and PLGA during formation of the nanoparticles. The zeta potential measured for the PLGA-TPGS polymeric nanoparticles was -31.4 mV. In theory, nanoparticles that are negatively do not attract electrostatic interactions with the cell membrane's negatively charged phospholipid elements as a result, probabilities of being cleared by macrophages are less likely. Zetasizer further confirmed the size distribution of PLGA-TPGS polymeric nanoparticles which was nanoparticle size of 186.9 nm and a small particle size distribution with a PDI of 0.157. The morphology of the PLGA-TPGS polymeric nanoparticles was analysed by SEM microscopy. The nanoparticle formulations were well distributed, had a regular spherical shape between 91nm and 200 nm in size, with a mean diameter of 186 nm. MXT release kinetics from PLGA-TPGS polymeric nanoparticles were profiled successfully, it displayed that MXT could be released up to 85% in gastrointestinal environment. The results specified above confirmed that the MTX polymeric nanoparticles polymer was successfully synthesized.

CHAPTER 4
PHASE 2: SYNTHESIS AND OPTIMIZATION OF THE SODIUM ALGINATE-GELATINE BIO-INK AS A 3D PRINTABLE MATRIX FOR NANOPARTICLE FIXATION

4.1 Introduction

The sodium alginate-gelatine (SA-GL) bio-Ink was developed using a modified method first reported by Luo and co-workers, (2018). The optimising templates and final matrix were printed using an Envisiontec 3D Bioplotter (Figure 4.1) with a temperature-controlled printing platform.

Gelatine (GL) is a collagen derived, water soluble protein which is used in many different pharmaceutical applications. GL-based hydrogels are well suited to 3D printing (3DP) and was therefore selected as a primary polymer framework due to its previously demonstrated thermolability, biocompatibility, biodegradability, non-immunogenicity and structural integrity (Shin & Kang, 2018; Wang, et al., 2017).

Sodium alginate (SA) is a polysaccharide derived from the cell walls of brown algae and is a powerful thickening, stabilizing, and gel-forming agent used in the food and pharmaceutical industries. SA is also biocompatible and versatile which makes it ideal for use in the design of drug delivery systems (Sosnik). SA forms a gel when placed in contact with divalent cations such as Ca^{2+} due to the formation of a net-like structure that results from crosslinking. Santos de Laia and co-workers (2014) demonstrated that the physicochemical properties of the crosslinked SA were enhanced.

In order to benefit from the individual properties of SA and GL this phase of the project focused on co-fabricating the two polymers to form a liquefied gel at room temperature making it suitable as a bio-ink. Heat sensitive drugs that may be degraded by high printing temperatures can be printed using a SA-GL bio-ink base to maintain drug stability. (Schütz, et al., 2017; Pietrzak, et al., 2015). Therefore, this bio-ink will also be suitable to fixate the MTX-loaded TPGS-functionalized PLGA NPs within the 3DP matrix.

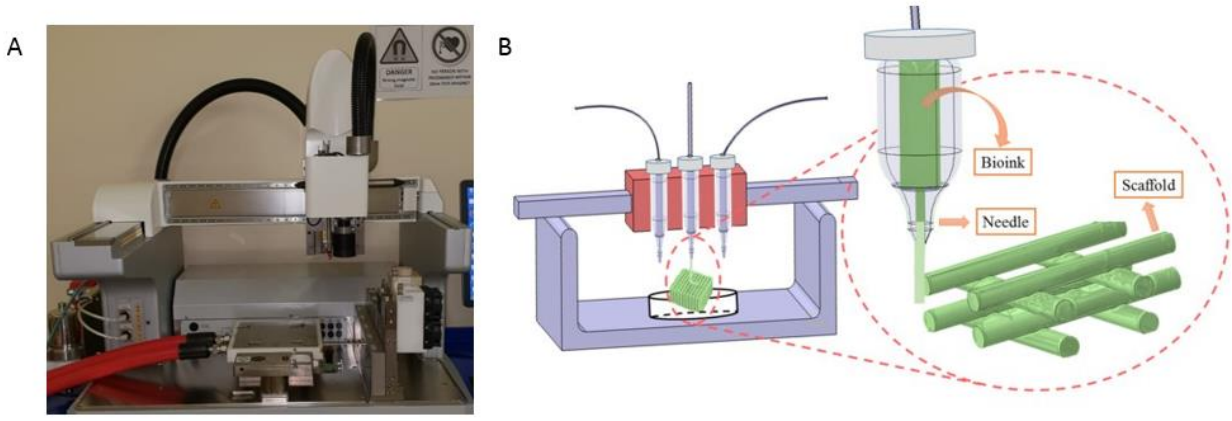


Figure 4. 1 Image (A) and schematic diagram (B) of 3D-Bioplotter, a versatile rapid prototyping tool (Naghieh, 2018).

Bioprinting is a recent technology for creating bio-artificial materials of a complex three-dimensional (3-D) structure, with high-precision spatial shape (Sun). In this chapter, templates of 3D-Bioplotter are optimised and validated so that the tablet delivery system could be printed using a temperature-controlled printing platform (Figure 4.1). Sodium Alginate and Gelatine are both economic and readily available (Schütz et al., 2017; Pietrzak et al., 2015). Alginate and Gelatine both form a liquefied gel at room temperature and thus are able to be used as a bio-ink at low temperatures. Temperature sensitive drugs that may be destroyed by high printing temperatures can be printed by using a bio-ink Alginate and Gelatine hydrogel without destroying its activity (Schütz, et al., 2017; Pietrzak, et al., 2015).

4.2. Materials and Methods

4.2.1 Materials

Alginic acid sodium salt from brown algae (Sodium Alginate), Methotrexate, Phosphate buffered saline, Gelatine Powder, Calcium Chloride dehydrate were purchased from Sigma (Sigma-Aldrich, Missouri, USA). All of the reagents procured were of the highest analytical grade.

4.2.2 Optimisation of Printing Parameters

Several factors are important in producing the optimal printed tablet. The printing ink was optimised by using various formulations of sodium alginate and gelatine under controlled conditions to determine the most accurate combination. The optimum printing parameters were obtained by using various tests for printing head temperature, platform temperature, printing precision tip size, printing pressure, pre-flow delay, post-flow delay, time between

layers, and printing speed. These tests with results outlined are discussed in the following chapters.

4.2.3 Printability and optimisation of Sodium Alginate Gelatine Bio-ink

Sodium alginate gel solutions of 3%, 5%, 8% and 10% was prepared by mixing 100 mL de-ionized ultrapure water with Sodium Alginate powder. The mixture was stirred on a magnetic stirrer for 1 hour. The mixture was then placed in the fridge at 4 °C for 24 hours to obtain a smooth homogenous gel. Gelatine gel solutions of 5%, 8% and 10% were mixed in warm phosphate buffered saline preheated to 60 °C on a magnetic stirrer for 30 minutes. The sodium alginate-gelatine printing ink was then prepared using 50 mL of warmed sodium alginate gel and 50 mL of warm gelatine mixture at different concentrations, the sodium alginate gelatine mixture was kept at a temperature of 60 °C. Previous studies have shown that maintaining gelatine gel at a stable high temperature prior to cooling increases strength and rigidity (Fonkwe, Narsimhan and Cha). It was hypothesised that a higher concentration of gelatine increases the solidity of the devices after printing and prior to crosslinking in $CaCl_2$, hence combinations of mixtures were tested with higher concentrations of gelatine than sodium alginate.

4.2.4 Optimum Hydrogel printable ink of Sodium Alginate/ Gelatine

To evaluate the printing accuracy of different concentrations of printing ink, a 17 mm diameter x 3 mm (height) round template was designed. The different concentration of bio-inks were loaded into a 30 mL plastic syringe. Three spherical tablet-shaped devices were printed with each bio-ink all using a printing speed of 35.0 mm/s with a stainless steel 0.25 mm precision tip. The minimum pressure that constant extrusion occurred was selected. Printed devices were measured with a calliper and the area of the devices calculated:

$A = \pi r^2$ ..... Equation 1

Printing accuracy was then determined by analysing the actual area of the device, A_i (X mm^2) against the designed area, A (227 mm^2), using the following equation (Di Giuseppe, et al., 2018):

$Printing\ Accuracy\ (\%) = [1 - |\frac{A_1 - A}{A}|]$x 100.....Equation 2

4.2.5 Determination of the effect of needle gauge on 3D printing accuracy

Multi-purpose stainless steel precision tip needles were used for 3D printing of the matrices. The optimized needle size for 3D printing of the bio-ink was determined by conducting

printability tests using needles with a range of gauge sizes (G). Needle diameters were as follows (ID = inner diameter): 20 G (ID = 0.61 mm); 21 G (ID = 0.51that included: 22G (ID = 0.41 mm); 25G (ID = 0.25 mm) and 27G (ID = 0.20 mm). Visual examination of the 3D printed strands was used to determine the optimal printing pressure for each needle size. The initial printing pressure was set at 500kPa and the pressure during printing varied until a continuous uniform strand was printed. The minimum pressure that resulted in constant extrusion was then selected. The printing speed for each matrix was set at 30mm/s. To evaluate the printing accuracy between the different needle sizes, a 15x 15 x 3 mm square template was designed, and square-shaped matrices were printed using stainless-steel precision tips. The printed matrices were measured with a digital calliper and the matrix area was calculated using Equation 3.

$Volume = length\ x\ width$……Equation 3

4.2.6 Crosslinking of sodium alginate

Sodium alginate forms a crosslinked gel when added to a solution of calcium chloride, due to the cross-linker through the exchange of sodium ions (Na^{+}) and calcium ions ($Ca^{2+).}$ (Figure 4.2).

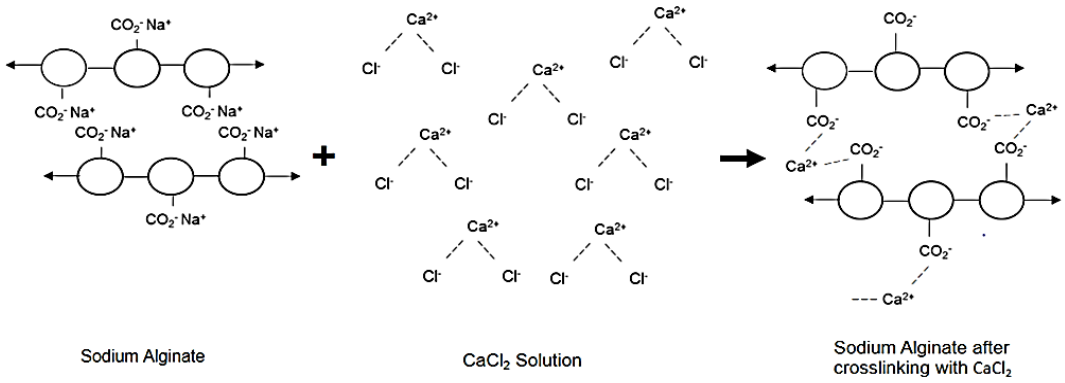


Figure 4. 2 Sodium alginate gelation through crosslinking by exchange of sodium ions (Na+) and calcium ions (Ca^{2+}).

4.2.7 Temperature induced Crosslinking of Gelatine

Park Heon, 2020 reported the transition from solution to gel to be 10 % gelatine solution at 29 °C after cooling from 45 °C for approximately 5 minutes. Time also plays a role in the gelation of a gelatine solution and as time increases, the gelatine solution is more likely to transition to gel at lower temperatures. Printing head temperatures were set at either 30, 35 and 40 °C (maximum head temperature 40 °C) to determine the temperature at which the printing ink does not transition to gel within the cartridge during printing. Printing ink was loaded into a cartridge and used to print at 5, 10, 15, 20, 30, 45, 60, 90 and 120 minutes (min) through a 0.25 mm needle at a pressure of 2000 kPa until the ink gelation had occurred sufficiently to

prevent extrusion. The printing needle was cleaned between each printing session to prevent possible clogging.

4.2.8 Determination of optimum printing speed and pre- and post-flow delay times

The most precise 3D Printing of Sodium Alginate-gelatine nanoparticle formulation was at a printing speed of 25.0, 30.0, 35.0 and 40.0 mm/s at a pressure of 1.4 KPa bar with a stainless steel 0.25 mm precision tip. Pre- post-flow delays were set at intervals of 0.01 seconds and printed layers observed to determine the optimum pre- post-flow delays which resulted in the layers not exhibiting any gaps.

4.3 Results and Discussion

4.3.1 Optimisation of Sodium Alginate/ Gelatine Printing Ink

Three matrices round devices were 3D printed at with every varying concentrations of bio-inks as listed in Table 4.1, using a printing speed of 35.0 mm/s with a stainless steel 0.25 mm precision tip. The minimum pressure that constant extrusion occurred was selected.

Table 4.1 shows the different combinations of sodium alginate and gelatine bio-printing ink prepared. The results revealed show that the highest printing accuracy was obtained with 8% sodium alginate and /10% gelatine as the bio-gelatine ink.

Table 4. 1 Printing accuracy of different concentrations of Sodium Alginate/ Gelatine in printing ink.

SA-GL Blend	Printing Pressure (kPa)	Matrix Size (mm^2) *	Printing Accuracy (%)
3%SA-5%GL	800	175.12 ± 15.03	77.15 ± 6.62
5%SA-5%GL	800	197.74 ± 21.05	87.11 ± 9.27
5%SA-8%GL	900	247.23 ± 24.82	91.09 ± 8.91
8%SA-10%GL	1300	219.92 ± 5.44	96.88 ± 2.40
10%SA-10%GL	1500	250.65 ± 6.35	89.58 ± 2.80

* n = 3

Increasing the concentration of SA resulted in higher printing accuracy with bio-ink blends of 8% SA and 10% GL producing the best accuracy at 96.88%. The same was observed when the concentration of GL was increased, with no significant difference observed between concentrations of 5% and 8% GL ($p>0.05$). Higher (10%) and lower (3%) concentrations of SA significantly reduced the printing accuracy for low (5%) and high (10%) concentrations of GL (**Error! Reference source not found.**).



Figure 4. 3 Images of typical 3D printed SA-GL tablet-shaped matrices produced using a 3D Bioplotter in the least and most favourable concentrations: *a. Least favourable printing ink (5%SA-8%GL) and b. Most accurate printing ink (8%SA-10%GL)*

4.3.2 The influence of printing needle size on 3D printing accuracy

The printing accuracy (%) of varying needle sizes was determined as described in section 4.2 by analysing the average area of three square 15 mm x 15 mm x 3 mm printed matrices per needle size. The results indicated that the highest printing accuracy (including a 15 sec dwell time between layers) was achieved using a 25G needle (**Error! Reference source not found.**).

Table 4. 2 Assessment of 3D printing needle size and printing accuracy (%) of matrices

Needle Gauge (G)	Needle Inner Diameter (mm)	Optimal Printing Pressure (kPa)	Printing Accuracy (%)
20	0.61	100	73.3
21	0.51	300	76.7
22	0.41	800	87.9
25	0.25	1400	95.6
27	0.20	2000	82.3

4.3.3 Optimisation of crosslinking time of Sodium Alginate-Gelatine devices in $CaCl_2$

To further strengthen after 3D printing the tablets were transferred to a deep well petri dish and covered with 3 mL of 2% $CaCl_2$ solution for 15 minutes. A study showed that crosslinking of the sodium alginate in the 3D printed devices significantly increases the hardness. The optimum crosslinking time determined was 15 minutes of immersion in $CaCl_2$. (Di Giuseppe, Law and Webb). The device was removed from the $CaCl_2$ solution and placed in a petri dish to dry at 4 °C for 1 hour.

4.3.4 Determination of optimum printing temperature

At 30 °C the printing ink was too thick to be extruded after 15 minutes. At 35 °C the printing ink could be extruded for a maximum of 90 minutes. The printing ink remained fluid at 40 °C for more than 2 hours and printing was conducted with the printing head set at this temperature. The results are summarised in table 4.3.

Table 4. 3 Extrudability of printing ink at different temperatures

Extrusion at:	5 min	10 min	15 min	20 min	30 min	45 min	60 min	90 min	120 min
30 °C	✓	✓	×	×	×	×	×	×	×
35 °C	✓	✓	✓	✓	✓	✓	✓	×	×
40 °C	✓	✓	✓	✓	✓	✓	✓	✓	✓

The printing platform temperature was reduced to 0 °C since this was an ideal temperature to ensure rapid cooling of the printing ink once printed. Temperatures lower than 0 °C was found to stimulate premature crosslinking within the printing syringe during printing due to the proximity of the syringe to the printing platform. This resulted in the printing ink solidifying within the tip of the printing syringe and the inability of the printing ink to be extruded from the syringe.

4.3.5 The influence of printing speed and pre- and post-flow dwell times on 3D printing accuracy

Using a 15 x 15 mm square template and printing 3 layers, a 3D printed matrix per printing speed was produced using printing speed of either 25 mm/s; 30 mm/s; 35 mm/s; and 40 mm/s (max) as described in section 4.2. The best printing speed was established as 35mm/s (**Error! Reference source not found.**). A pre- and post-flow dwell time of 0.05 seconds was found to be the most accurate to adjust appropriately for bio-ink flow lag.

Table 4. 4 Influence of 3D printing speed on printing accuracy

Printing Speed (mm/s)	Printed Matrix Size (mm^2)	Printing Accuracy (%)	Visual Inspection
25	N/A	N/A	Bio-ink was viscous and L2 resulted in printing needle extrusion into L3.
30	262	84	Bio-ink was over-extruded
35	227	99	Matrix was well formed with no structural defects
40	212	94	Matrix had several structural defects
45	N/A	N/A	Matrix had several structural defects and was no capable of L formation

4.3.6 The influence of temperature on 3D printing accuracy

A bio-ink blend comprising 8% SA and 10% GL was loaded into a 3D printing cartridge and loaded into the 3D Bioplotter. Three layers of the bio-ink were printed using a 15 x 5mm square template at 5; 10; 15; 20; 30; 45; 60; 90; and 120 minutes through a 0.25 mm needle at a pressure of 2000 kPa. This process was repeated three times (N=3) for printing cartridges set at 30 ˚C; 35 ˚C and 40˚C. The results are summarised in T**Error! Reference source not found.** and showed that at 30°C the bio-ink was too viscous to be extruded after 15 minutes. At 35°C the bio-ink was extruded for a maximum of 90 minutes and it remained fluid at 40 °C for >2 hours. Therefore, all subsequent 3D printing was undertaken with the printing cartridge set to 40˚C

4.3.7 Optimisation of the ionic crosslinking time of SA-GL matrices

The optimum crosslinking time was determined to be 15 minutes of immersion in $CaCl_2$. The matrix was removed from the $CaCl_2$ solution and placed in a petri dish to dry at 4 °C for 1 hour. The resulting devices were found to be uniform; round; and had good stability (

).

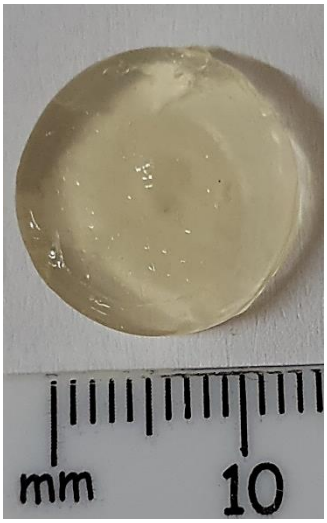


Figure 4. 4 Dried 3D printed sodium alginate-gelatine hydrogel devices following temperature and chemical crosslinking in $CaCl_2$

4.4 Concluding Remarks

In Phase 2 of this study an optimised 3D printable bio-ink was developed with the most accurate 3D printing parameters determined for fabricating the SA-GL tablet-like matrices. Varying combinations of SA-GL bio-inks were tested to determine the most efficient combination for 3D printing. The highest printing accuracy value was obtained from a bio-ink comprising 8% SA and 10% GL. This combination was used further in Phase 3 of this study to fixate the MTX-loaded TPGS-functionalized PLGA NPs within an oral tablet-like matrix.

CHAPTER 5
PHASE 3: DESIGN AND SYNTHESIS OF AN ORAL CHEMOTHERAPEUTIC 3D PRINTED NANOCOMPOSITE HYDROGEL TABLET

5.1 Introduction

Cancer is a public health concern and cause of death globally (Rebecca L. Siegel). Cancer is a name given to numerous related diseases that are responsible for breaking down the biological order in the body. Various cancer cells divide, replicate and metastasize into the surrounding tissues (Weinberg). Cancer can localise in almost every part of the body such as lung, gastrointestinal tract, central nervous system, breast in women and prostate in men (Leppert, 2016). One of the major concerns with treatment of cancer is that majority of therapeutic agents target healthy cells and cancerous cell. The other challenge is that cancer may localise in organs that are well protected by plasma membranes and therapeutic agents may be highly limited to penetrate through and reach the target sites (José M. Morachis). Methotrexate (MTX) is one of the extensively used and studied antineoplastic agents (Widemann, 2006). MTX can be administered *via* oral, subcutaneous, or intramuscular routes. However, in the conditions of chronic therapies, the oral administration is the preferred route of administration (Christophe). Furthermore, there are numerous factors that reduce therapeutic agent absorption from the gastrointestinal tract and lead to lower bioavailability in blood stream. To circumvent these factors, Poly Lactic-co-Glycolic Acid (PLGA) nanoformulations can be used to control drug release due their biocompatibility and biodegradability and are also approved by Food and Drug Administration (FDA) for therapeutic applications (Siegel et al., 2011). In addition, it has been reported that D-α-tocopheryl polyethylene glycol succinate (TPGS) act as P-glycoprotein inhibitor to reduce drug efflux. Study conducted by Yung et al., 2008 showed that PLGA nanoformulations with TPGS results in higher cellular uptake compared with nanoformulations without TPGS (Yung et al., 2008). In the present study, nanoformulations were incorporated into hydrogels to enhance the mechanical properties and sustain release chemotherapeutic agent. Sodium Alginate-Gelatine Hydrogels were used as printable inks to formulate an oral device that is incorporated with PLGA-TPGS nanoformulation. Hydrogels are environmentally sensitive and have a tendency to respond to changes in pH, temperature, or the metabolite concentration to release their drug payload (Ghasemiyeh et al., 2019). However, alginate have good pH stability that ranges between 3 to 10 (Ferreira et al., 2017). Hence, alginate hydrogels have potential for the development of drug delivery systems that can be applied at low pH environment (Ferreira, et al., 2017). However, the drawbacks of hydrogels like alginates are large pore sizes and low mechanical strength that often result in burst release in extreme pH environment due to

protonation and relaxation of crosslinked chains (Rizwan et al., 2017). These alginate hydrogel flaws reduce the capabilities to control and sustain chemotherapeutics release over time compromising critical parameters in clinical applicability. (Ferreira et al., 2017). Furthermore, gelatin are well known as drug delivery carriers and have demonstrated natural versatility and flexibility that enables the loading of charged molecules. Marco Sontoro (2015) indicated that gelatine isoelectric point can be modified in order to maximize chemotherapeutic loading efficiency by using either basic or acidic treatment (Santoro, et al., 2015). In the present study, a combination of alginate-gelatine hydrogel printable ink was utilized to formulate an oral drug delivery device using 3D-Bioplotter. In previous studies polymeric alginate-gelatine has been employed as a tablet replacement material with beneficial properties (Saha et al., 2013). The 3D-Bioplotter is a rapid-prototyping system that facilitate the design detailed scaffolds for the control of mechanical properties and pore structures for required construct (Son et al., 2009). The automated 3D-Bioplotter was used to achieve the purpose of this study, which was to fabricate and characterise 3D printed oral drug delivery devices using Sodium Alginate-Gelatine printing ink incorporated with Methotrexate-loaded in polymeric TPGS-PLGA nanoparticles.

5.2 Methods

5.2.1 Materials

Alginic acid sodium salt from brown algae (Sodium Alginate), Methotrexate, Phosphate buffered saline, Gelatine Powder, Calcium Chloride dehydrate were purchased from Sigma (Sigma-Aldrich, Missouri, USA). All of the reagents procured were of the highest analytical grade.

5.2.2 Preparation of Sodium Alginate-Gelatine Nanoparticle Formulation Printing Ink

The Sodium Alginate-Gelatine (8% sodium alginate and 10% gelatine (w/v)) was stirred for 30 min at 60°C. Polymeric combination of TPGS and PLGA containing 50 mg of MXT was dispersed into the 50 mL of Sodium Alginate-Gelatine under constant stirring at 60°C for 30 min to form nanocomposite hydrogels. The Sodium Alginate-Gelatine Nanoparticle Formulation printing ink was formed.

5.2.3 Design of 3-D Printed Tablets

Changing the shape and dimensions of a tablet can alter the way patients perceive medication and lead to greater willingness to adhere to treatment. Several studies have shown that there is a link between the shape of oral medication tablets and the patient's perception of the medication. Spherical tablets were preferred over angular tablets and were regarded as easier to swallow. Patient well-being can be increased by using shape and colour of pills to change

how they perceive the overall sensory experience. (Wan et al., 2015; Lajoinie et al., 2016; Ternik, et al., 2018). Therefore, the tablets in this study were designed to be disk-shaped tablets with a mean diameter of 15.0 mm and a height of 3.60 mm.

The average volume of the tablets was calculated using the following formula:

$$Volume = \pi r^2 \times height$$ ..... Equation 4

5.2.4 Thermal Analysis of 3D Printed Tablets

Thermogravimetric analysis (TGA) was performed on the Sodium Alginate-Gelatine Nanoparticle Formulation for oral drug delivery and blank sodium alginate-gelatine printing ink without nanoparticle formulations. Samples were heated at 10 °C/min in open aluminium pans, using nitrogen as a purge gas (flow rate of 25 mL/min). The percentage mass loss and/or onset temperature was calculated.

5.2.5 *In Vitro* Analysis of the 3D Printed Sodium Alginate-Gelatine Hydrogel-Nanoparticle Formulation for Oral Drug Delivery

Ultraviolet–visible spectroscopy (UV-Vis) is the absorption spectroscopy in the region of ultraviolet light i.e., ultraviolet-visible region. The reflectance and absorbance in this region have an effect on the apparent colour of the elements involved. UV-Vis spectroscopy is used to measure the maximum wavelength of a therapeutic and draw calibration curve for determination of the release profile. In vitro drug release studies were performed at both gastric and intestinal pH conditions. The 3D Printed Sodium Alginate-Gelatine Nanoparticle Formulation Oral Drug Delivery Devices were placed in 10 mL of simulated gastric (pH 1.2) and intestinal (pH 6.8) phosphate-buffered in saline for a duration of 0 to 2.5 h. Samples were incubated during the release duration using an Orbit shaker incubator (LM-530-2, MRC Laboratory Instruments LTD., Hahistadrut, Holon, Israel) at 37 ± 0.5 °C and 30 rpm. Samples (0.5 mL) were withdrawn from simulated gastric release buffer every half an hour for 2.5 h simulated gastric samples, and at 30 min, then hourly for the first 12 h and at 24 h. The withdrawn liquid was replaced by a 0.1mL control solution at 37 °C for compensation. All extracted samples were filtered using a .45 Millipore Millex filter and stored at 4–8 °C. Ultraviolet–Visible spectroscopy was employed to determine the concentration of methotrexate.

5.3 Results and Discussion

5.3.1. 3-D Printing of Sodium Alginate-Gelatine Hydrogel Nanoparticle Formulation (Oral Chemotherapeutic Delivery System)

Sodium Alginate-Gelatine hydrogels were stirred and warmed at 60 °C then the polymeric PLGA-TPGS nanoparticles loaded with MXT were incorporated to form nanocomposite hydrogel system. The Sodium Alginate-Gelatine Hydrogel Nanoparticle Formulation printing ink was then formed. Ten tablets of Sodium Alginate-Gelatine Hydrogels Nanoparticle Formulation were printed using optimised printing parameters obtained (Figure 5.1). The printing platform was set to 0 °C to ensure that the gelatine temperature induced hydrogen bond crosslinking as soon as possible after printing, thereby increasing the stability of the structure (Zhao, 2015; Xing, 2014). The syringe temperature was set to 40 °C to prevent any crosslinking prior to printing. The Inner structure of the tablet was formed by setting the 3D-Bioplotter to print at 90° angles at a printing distance of 0.3 mm and printing speed of 35 mm/s. This ensured that the tablet had a solid infill. Layer height was set at 0.22 mm with a total of 13 layers printed. The time between layers was set at 15 seconds to allow adequate crosslinking to occur.

After printing, Sodium Alginate-Gelatine Nanoparticle Formulation tablets were placed in a round-bottom petri dishes covered with 2% Calcium-Chloride solution for 30 minutes to facilitate cross-linking of the sodium alginate. Ten tablets of Sodium Alginate-Gelatine Nanoparticle Formulation were printed and had an average weight of 606 mg ± 9 mg. The dimensions of the Sodium Alginate-Gelatine Nanoparticle Formulation had an average height of 3.56 mm and average diameter of 14.98 mm. The average volume of the tablets was calculated as 626.83 mm^3 and the tablets had an average drug load of 0.627mg of MTX.

5.3.2. Determination of thermal stability of the Sodium Alginate-Gelatine Nanoparticle Formulation

TGA was used to distinguish and quantify the chemical or physical variations that occur upon heating a sample. TGA measures the quantity and degree of weight transformation of a substance in relation to a controlled temperature or time (Figure 5.1 & 5.2). This information is then interpreted to predict the thermal stability of a substance and its components up to temperatures as high as 1000 °C by evaluating the weight changes caused by evaporation, dehydration, oxidation and decomposition. There may be multiple stages of multiple weight loss phases which signify the presence of several constituents in a substance (Stodghill). The TGA curve shows that the Sodium Alginate-Gelatine printing ink loses 14.8% of its weight at 200 °C. This initial weight loss may be due to evaporation of bound water. Further 35.9 %

weight loss was observed between 200 °C and 280 °C. A further 13.1% weight loss was recorded between 280 °C and 600 °C, and the total value of weight loss reached 79.4% at 900 °C. The TGA plot of Sodium Alginate-Gelatine Nanoparticle Formulation shows a slightly different trend compared to the Sodium Alginate-Gelatine ink. Yuandong (2010) reported a polymeric PLGA-TPGS to contribute to thermal degradation properties. TGA analysis was performed on the synthesized PLGA-TPGS copolymer in order to investigate its thermal property and it was established that the sudden reduction in mass was between 215 °C and 300 °C (Yuandong, et al., 2010). In this study, Sodium Alginate-Gelatine Nanoparticle Formulation did not show this sudden reduction in weight between 240 °C and 260 °C. At 200 °C, the Sodium Alginate-Gelatine Nanoparticle Formulation lost 9.2% of their weight. Between 200 °C and 280 °C, there was a further weight loss of 18.3%. At the final temperature of 900 °C, the total weight loss reached was 75.6%. The results suggested that the Sodium Alginate-Gelatine Nanoparticle Formulation had higher thermal stability due to the encapsulated drug-loaded nanoparticles.

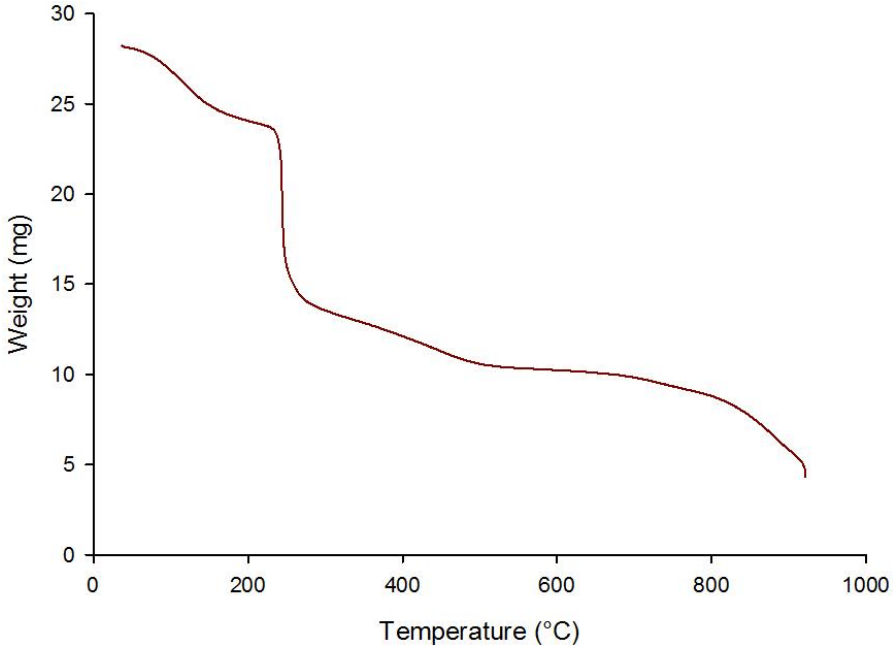


Figure 5. 1 Thermogravimetric (TGA) analysis of Sodium Alginate-gelatine printing ink (as prepared; prior to 3D printing and thermal and chemical crosslinking)

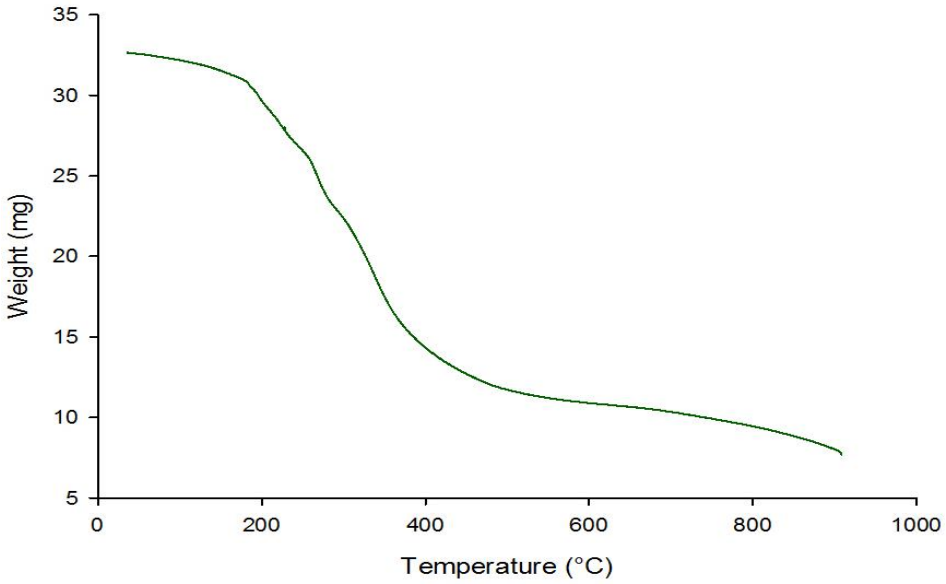


Figure 5. 2 Thermogravimetric (TGA) analysis of 3D Printed Sodium Alginate-Gelatine Nanoparticle Formulation (Oral Chemotherapeutic Delivery System).

5.3.3 Drug release profiles of the Sodium Alginate-Gelatine Hydrogel Nanoparticulate system

To determine the Ultraviolet (UV) absorbance of MTX, a solution of MTX in pH 6.8 phosphate-buffered saline with concentration of 10-100 µg/mL was prepare. The concentration of the drug was measured against absorbance and a standard calibration curve was obtained with a linear equation: $y = 0.0004X + 0.0188$ with R^2 of 0.9987.

In vitro release of Sodium Alginate-Gelatine MTX loaded-Nanoparticulate formulation was conducted in pH 6.8 and pH 1.2 to simulate the gastrointestinal environment with sustained release patterns in pH 6.8 buffer observed compared to pH 1.2 buffer (Figure 5.3). While in pH 1.2, the drug showed an initial burst release in the first 60 minutes and then after 60 to 150 minutes, there was also stable sustained release of MTX (Figure 5.3). These results also indicate that the drug release was accelerated in gastric acidic environment validating that the majority of the MTX was released prior to entering the intestinal tract. Hydrogels have characteristics that are similar to tissues but may suffer from burst release and rapidly diffusion of chemotherapeutics from the polymer matrix due to pH-sensitivity and swelling behaviour. These gels can be investigated by monitoring the deflection of hydrogel-coated micro-cantilevers due to sensitive and repeatable response to solution pH (Mao et al., 2006). The swelling of the hydrogel was mainly as a result of chain relaxation of gelatine drug complexes due to protonation of free amino groups in gelatine. The main advantage of hydrogels is their extent of drug release that can be controlled and in polymeric nanoparticles complexed within

hydrogels, the drug release duration can be significantly prolonged resulting in enhanced drug bioavailability (Sharpe et al.,2014).

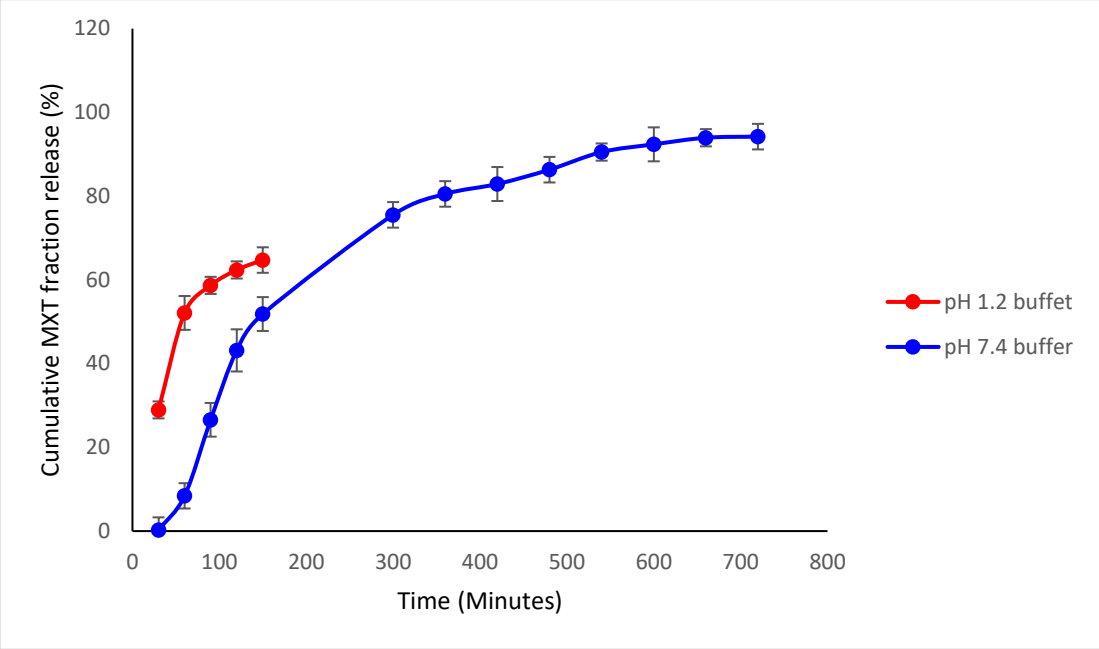


Figure 5. 3 *In vitro* MTX release from Sodium Alginate-Gelatine Nanoparticle Formulation conducted in pH 1.2 and pH 7.4 buffer (n=3, mean ± SD).

5.4 Concluding Remarks

The incorporation of PLGA-TPGS polymeric nanoparticles in Alginate-Gelatine hydrogels to form Oral Drug Delivery system was successfully performed and characterized. The results also indicated that the high accuracy of the 3D printed hydrogel/nanocomposite system (including 15 sec pauses between layers) was achieved using a 25 G needle with inner diameter of 25 mm, optimal printing pressure was1400 kPa and 95% printing accuracy. Ten Sodium Alginate-Gelatine Nanoparticle Formulations (Oral Drug Delivery system) were successfully printed with an average weight of 606 mg ± 9 mg. TGA analysis indicated that Sodium Alginate-Gelatine Nanoparticle Formulations had a gradual loss of weight from 200 ˚C. UV absorbance of MTX obtained at a drug concentration of 10-100 µg/mL resulted in a linear response of $y = 0.0004X + 0.0188$ with R^2 of 0.9987. Sodium Alginate-Gelatine Nanoparticle Formulation in pH 6.8 buffer demonstrated sustained release patterns whilst, at pH of 1.2, the drug showed an initial burst release in the first 60 minutes due to chain relaxation of hydrogel drug complexes caused by protonation of free amino groups in hydrogels. The effective encapsulation of PLGA-TPGS polymeric nanoparticles into Alginate-Gelatine hydrogel provides a good insight for future applications in controlled drug release systems.

CHAPTER 6
CONCLUSION

6.1 Conclusion

This study gives emphasis to the need for alternative advanced drug delivery approaches to halt and treat the spread of cancer. The primary objective of cancer diagnosis and treatment programmes are to cure and to prolong life of patients whilst ensuring the best quality of life for cancer survivors. Administering chemotherapeutics *via* oral route is preferred compared to intravenous administration due to better patient compliance and ease of administration. It has been reported that there are numerous challenges that comes with oral administration, such as poor aqueous solubility, poor enzymatic stability, gastrointestinal pH and efflux pumps that are located in gastrointestinal environment. There was interest to develop chemotherapeutics that can either passively or actively target cancerous cells or reduce adverse side effects whilst improving therapeutic efficacy. A multifunctional chemotherapeutic drug such as Methotrexate does not penetrate efficiently through plasma membrane barriers. However, to target tumours in well protected organs such as brain, it was necessary to administer Methotrexate by high-risk intrathecal injections. It has been reported that Methotrexate loaded PLGA-TPGS polymeric nanoparticles have an ability to penetrate through tight plasma membranes and show enhanced therapeutic efficacy on cancer cells. Furthermore, 3D printing is an evolving technology generation with numerous applications in generating desired structures in an attempt to systematically halt human diseases such as cancer. Automated 3D bioprinters are a fairly new technology that provides high reproducibility and precise control in production desired structures of delivery devices.

The folic acid targeting abilities of Methotrexate can also improve the effectiveness and cell targeting of the treatment and should be a subject of further study. Numerous studies have demonstrated the PLGA nanoparticle systems as a promising chemotherapeutic carrier for tumour targeted sites. In this research PLGA-TPGS Methotrexate loaded polymeric nanoparticles were synthesized. The PLGA-TPGS polymeric nanoparticles were characterized using FTRI technique and displayed a comparable peak to the PLGA and Methotrexate. It was also concluded that the nanoparticle formulations have similar chemical composition suggesting there was no significant chemical interaction between the functional groups of Methotrexate and PLGA during formation of the nanoparticles. The zeta potential measured for the PLGA-TPGS polymeric nanoparticles was -31.4 mV. In several studies suggested negatively nanoparticles do not electrostatically interact with the cell membrane that is negatively charged by phospholipid elements therefore, chances of being cleared by

macrophages are low. With the aid of Zetasizer technique the size distribution PLGA-TPGS polymeric blend nanoparticles and zeta potential was confirmed to be nanoparticle size of 186.9 nm and a small particle size distribution with a PDI of 0.157. The morphology of the PLGA-TPGS polymeric nanoparticles was investigated by SEM microscope technique. The PLGA-TPGS polymeric nanoparticles were well distributed, had a regular orbicular shape, and were between 91nm and 249 nm in size, with a mean diameter of 150 nm. The results specified above advocate that the Methotrexate polymeric nanoparticles polymer was successfully synthesized.

Several benefits of nanoparticles in drug delivery to tumour has been well researched and reported in previous studies. The controlled dosing and targeted delivery could show great promise in addressing the challenges experienced in delivering chemotherapeutic medicines. In this study the inclusion of PLGA-TPGS polymeric nanoparticles in Alginate-Gelatine hydrogels was successfully performed and characterized. Ten Sodium Alginate-Gelatine Nanoparticle Formulation Oral Drug Delivery Devices were successfully printed with an average weight of 606 mg ± 9 mg. TGA analysis indicated that Sodium Alginate-Gelatine Nanoparticle Formulation Oral Drug Delivery Devices did not show sudden reduction in weight at any temperature however, there was a gradual loss of weight from 200 ˚C. UV absorbance of MTX obtained at a drug concentration of 10-100 µg/mL resulted in a linear response of $y = 0.0004X + 0.0188$ with R^2 of 0.9987. Sodium Alginate-Gelatine Nanoparticle Formulation Oral Drug Delivery Devices in pH 7.4 buffer demonstrated a sustained release pattern whilst, at pH of 1.2, the drug showed an initial burst release in the first 60 minutes due to chain relaxation of hydrogel drug complexes caused by protonation of free amino groups in hydrogels. Methotrexate-loaded in polymeric TPGS-PLGA nanoparticles incorporated into Sodium Alginate-Gelatine oral drug delivery devices and were successfully developed in this study. The method developed for producing chemotherapeutics delivery devices is significant, adaptable, versatile, and easily adjustable to meet precise patient requirements. 3D printing can be used at any physician practice and is cost-effective way of producing medicines and to overcome the problems associated with mass produced products. A novel 3D printed tablet, loaded with methotrexate polymeric nanoparticles, for oral drug delivery was designed and analysed. The 3D printed devices loaded with nanoparticles show great potential in the development of personalised medicine with the benefits of nanoparticle technology.

6.2 Future Recommendations

The toxicity of Sodium Alginate-Gelatine Nanoparticle Formulation Oral Drug Delivery Devices is also unknown and the cytotoxicity tests in mammalian cells needs to be conducted in future studies. The inclusion of polyelectrolyte complexes in hydrogels could be beneficial since, it

has a potential to prevent the burst and control the drug release under low pH environment. The study conducted paves way for future studies using Sodium Alginate-Gelatine Nanoparticle Formulation in cancerous induced animal model to determine *in vivo* effect. In vivo models are the gold standard in preclinical evaluation of intestinal drug transport with intact physiological processes and disease features. A non-cell based model such as vesicle-based permeation assay (PVPA) which based on artificial biomimetic membranes provides a perfect tool to evaluate the passive intestinal absorption of the nanoparticles. PVPA has the benefits of being easy to use and has a high similarity with the biostructure of the intestinal Epithelium. Additionally, a cell-based model such as Transwell-based cell models can provide the perfect tool for studying transport mechanisms. (Xu, Shrestha and Preat). In vivo stability studies to determine the drugs stability in the hydrogel should also be conducted.

Future studies will also be inclusive of tissue pharmacokinetics profiles after oral administration in order to understand chemotherapeutics accumulation in tissues.

REFERENCES

1. Abitha Murugeshu, Carlos Astete, Claudia Leonardi, Timothy Morgan, Cristina M Sabliov. "Chitosan/PLGA Particles for Controlled Release of α-Tocopherol in the GI Tract via Oral Administration." *Nanomedicine* (2011): DOI: 10.2217/nnm.11.44.

2. AboulFotouh, Khaled, et al. "Role of self-emulsifying drug delivery systems in optimizing the oral delivery of hydrophilic macromolecules and reducing interindividual variability." *Colloids and Surfaces B: Biointerfaces* 167 (2018): 82 - 92.

3. Afshari, M, K Derakshandeh and L Hosseinzadeh. "Characterisation, cytotoxicity and apoptosis studies of methotrexate-loaded PLGA and PLGA-PEG nanoparticles." *Journal of Microencapsulation* 31.3 (2014): 239-245.

4. Akhand Pratap Singh, Arpan Biswas, Aparna Shukla, and Pralay Maiticorresponding author. "Targeted therapy in chronic diseases using nanomaterial-based drug delivery vehicles." *Signal Transduct and Target Therapy* (2019): doi: 10.1038/s41392-019-0068-3.

5. Alomari, M, et al. "Personalised dosing: Printing a dose of one's own medicine." *International Journal of Pharmaceutics* 494.2 (2015): 568-577.

6. Amani, Amin, et al. "Multifunctional magnetic nanoparticles for controlled release of anticancer drug, breast cancer cell targeting, MRI/fluorescence imaging, and anticancer drug delivery." *Journal of Drug Delivery Science and Technology* 49 (2019): 534-546.

7. Amjadi, Sajed, Hamed Hamishehkar and Marjan Ghorbani. "A novel smart PEGylated gelatin nanoparticle for co-delivery of doxorubicin and betanin: A strategy for enhancing the therapeutic efficacy of chemotherapy." *Materials Science & Engineering C* 97 (2019): 833-841.

8. Aquino, Rita Patrizia, et al. "Envisioning smart and sustainable healthcare: 3D Printing technologies for personalized medication." *Futures* 103 (2018): 35-50.

9. Bahrami, Behdokht, et al. "Nanoparticles and targeted drug delivery in cancer therapy." *Immunology Letters* 190 (2017): 64-83.

10. Bajetta E, Gevorgyan A, Mellstedt H. "National integration of European standards." *Annals of Oncology* 18 (2007): 969–970.

11. Bakarich, Shannon E, et al. "4D Printing with Mechanically Robust, Thermally Actuating Hydrogels." *Macromolecular Rapid Communications* 36 (2015): 1211-1217.

12. Beck, R.C C, et al. "3D printed tablets loaded with polymeric nanocapsules: An innovative." *International Journal of Pharmaceutics* 528 (2017): 268-279.

13. Beloqui, Ana, et al. "Nanostructured lipid carriers as oral delivery systems for poorly soluble drugs." *Journal of Drug Delivery Science and Technology* 42 (2017): 144 - 154.

14. "Cancer." 2018. *World Health Organisation.* 3 Jan 2020. <http://www.who.int/cancer/en/>.

15. Cerqueira, B B, et al. "Development of biodegradable PLGA nanoparticles surface engineered with hyaluronic acid for targeted delivery of paclitaxel to triple negative breast cancer cells." *Materials Science and Engineering* C.76 (2017): 993-600.

16. Chong Li, Jian cheng Wang, Yiguang Wang, Huileb Ga, Gang Weid, YongzhuonHuange, Haijun Yue, Yong Gane, Yongjun Wang, Lin Meig, Huabing Chenh, Haiyan Hui, Zhiping Zhang, Yiguang Jink. "Recent progress in drug delivery." *Acta Pharmaceutica Sinica B* 6.9 (2019): 1145-1162.

17. Christophe Leroux. "Polymeric micelles for oral drug delivery." *European Journal of Pharmaceutics and Biopharmaceutics* 2.76 (2010): 147-158.

18. Chua C.K, Wong C.H, Yeong W.Y. *Standards, Quality Control, and Measurement Sciences in 3D Printing and Additive Manufacturing*. 5th. London: Academic Press, 2017.

19. Clark, Elizabeth A, et al. "3D printing of tablets using inkjet with UV photoinitiation." *International Journal of Pharmaceutics* 529 (2017): 523-530.

20. Collnot, E, et al. "Influence of vitamin E TPGS poly(ethylene glycol) chain length on apical efflux transporters in Caco-2 cell monolayers." *Journal of Controlled Release* 111 (2006).

21. Conglian Yang, Tingting Wu, Yan Qi, and Zhiping Zhang. "Recent Advances in the Application of Vitamin E TPGS for Drug Delivery." *Theranostics* 8.2 (2018): 464–485.

22. Courtney R. Lynch, Pierre P. D. Kondiah, Yahya E. Choonara, Lisa C. du Toit, Naseer Ally and Viness Pillay. "Biomedical applications of hydrogels: A review of patents." *Frontiers in Bioengineering and Biotechnology* (2020): https://doi.org/10.3389/fbioe.2020.00228.

23. Daniel Eek, Meaghan Krohe,Iyar Mazar,Alison Horsfield,Farrah Pompilus,Rachel Friebe, and Alan L Shields. "Patient-reported preferences for oral versus intravenous administration for the treatment of cancer: a review of the literature." *Patient Prefer Adherence* 10 (2016): 1609–1621.

24. Date, A A, et al. "Mucus-penetrating budesonide nanosuspension enema for local treatment of inflammatory bowel disease." *Biomaterials* 185 (2018): 97-105.

25. Di Giuseppe, Michael, et al. "Mechanical behaviour of alginate-gelatin hydrogels for 3D bioprinting." *Journal of the Mechanical Behavior of Biomedical Materials* 79 (2018): 150-157.

26. Driscoll C.M.O, Griffin B.T. "Biopharmaceutical challenges associated with drugs with low aqueous solubility—The potential impact of lipid-based formulations." *Advanced Drug Delivery Reviews* 60.6 (2008): 617-624.

27. Du, X, et al. "Current development in the formulations of non-injection administration of paclitaxel." *International Journal of Pharmaceutics* 542 (2018): 242-252.

28. Dyson, Janet, et al. "Direct and indirect P-glycoprotein transfers in MCF7 breast cancer cells." *Journal of Theoretical Biology* 461 (2019): 239-253.

29. Echave E. M, Burgo C, Laura L. "Gelatin as Biomaterial for Tissue Engineering." *Current Pharmaceutical Design* 23.24 (2017): 3567-3584.

30. Fina, Fabrizio, et al. "3D printing of drug-loaded gyroid lattices using selective laser sintering." *International Journal of Pharmaceutics* (2018): 44-52.

31. Fonkwe, Linus G, Ganesan Narsimhan and Alice S Cha. "Characterization of gelation time and texture of gelatin and gelatin–polysaccharide mixed gels." *Food Hydrocolloids* 17 (2003): 871-883.

32. Fooroozandeh, Parisa and Azlan Abdul Aziz. "Insight into Cellular Uptake and Intracellular Trafficking of Nanoparticles." *Nanoscale Research Letters* 13 (2018).

33. Fulias, Adriana, et al. "Thermoanalytical and spectroscopic study on Methotrexate – active substance and tablet." *Digest Journal of Nanomaterials and Biostructures* 9.1 (2014): 93-98.

34. Gao, K and X Jiang. "Influence of particle size on transport of methotrexate across blood brain barrier by polysorbate 80-coated polybutylcyanoacrylate nanoparticles." *International Journal of Pharmaceutics* 310.1-2 (2006): 213-219.

35. Gaumet, Marie, et al. "Nanoparticles for drug delivery: The need for precision in reporting particle size parameters." *European Journal of Pharmaceutics and Biopharmaceutics* 69 (2008): 1-9.

36. Gaurav Tiwari, Ruchi Tiwari, Birendra Sriwastawa, L Bhati, S Pandey, P Pandey, and Saurabh K Bannerjee. "Drug delivery systems: An updated review." *International journal of pharmceutical investigations* 1.2 (2012): 2-11.

37. Ghandi, Sona and Indragit Roy. "Doxorubicin-loaded casein nanoparticles for drug delivery: Preparation, characterization and in vitro evaluation." *International Journal of Biological Macromolecules* 121 (2019): 6-12.

38. Goyanes, Alvaro, et al. "3D printing of modified-release aminosalicylate (4-ASA and 5-ASA) tablets." *European Journal of Pharmaceutics and Biopharmaceutics* 89 (2015): 157-162.

39. —. "Effect of geometry on drug release from 3D printed tablets." *International Journal of Pharmaceutics* 494 (2015): 657-663.

40. Groll J, Burdick J A , Cho D-W ,Derby B , Gelinsky M , Heilshorn S C ,. "A definition of bioinks and their distinction from biomaterial inks." *Biofabrication* (2018): https://doi.org/10.1088/1758-5090/aaec52.

41. Haseeb, Muhammad Tahir, et al. "Linseed polysaccharides based nanoparticles for controlled delivery of docetaxel: Design, in vitro drug release and cellular uptake." *Journal of Drug Delivery Science and Technology* 49 (2019): 143-151.

42. Hirenkumar K. Makadia., Steven J. Siegel. "Poly Lactic-co-Glycolic Acid (PLGA) as Biodegradable Controlled Drug Delivery Carrier." *Polymers* (2011): doi: 10.3390/polym3031377.

43. Honary, Soheyla and Foruhe Zahir. "Effect of Zeta Potential on the Properties of Nano-Drug Delivery Systems - A Review (Part 2)." *Tropical Journal of Pharmaceutical Research* 12.2 (2013): 265-273.

44. Horst, D.J. "3D Printing of Pharmaceutical Drug Delivery Systems." *Archives of Organic and Inorganic Chemical Sciences* (2018): 1-5.

45. J.W.Paxton. "Protein binding of methotrexate in sera from normal human beings: effect of drug concentration, pH, temperature, and storage." *Journal of pharmacological methods* 5.3 (1981): 203-213.

46. Jacques Jolivet, Kenneth H. Cowan, Gregory A. Curt, Neil J. Clendeninn, and Bruce A. Chabner. "The Pharmacology and Clinical Use of Methotrexate." *The new england journal of medicine* 309 (1983): 1091-1094.

47. Jayanta Kumar Patra, Gitishree Das, Leonardo Fernandes Fraceto,Estefania Vangelie Ramos Campos,Maria del Pilar Rodriguez-Torres, Laura Susana Acosta-Torres, Luis Armando Diaz-Torres, Renato Grillo, Mallappa Kumara Swamy, Shivesh Sharma,. "Nano based drug delivery systems: recent developments and future prospects." *Journal of nanobiotechnology* 16 (2018): 71.

48. Jiacheng Zhao, and Martina H. Stenzel. "Entry of nanoparticles into cells: the importance of nanoparticle properties." *Polymer Chemistry* (2018): https://doi.org/10.1039/C7PY01603D.

49. Jiang, Ke, et al. "A zirconium-based metal-organic framework with encapsulated anionic drug for uncommonly controlled oral drug delivery." *Microporous and Mesoporous Materials* 275 (2019): 229 - 234.

50. Jin, Yifei, et al. "Self-Supporting Nanoclay as Internal Scaffold Material for Direct Printing of Soft Hydrogel Composite Structures in Air." *Applied Materials and Interfaces* 9 (2017): 17456-17465.

51. Jin-Hyung Shim, Jong Young Kim, Min Park, Jaesung Park and Dong-Woo Cho. "Development of a hybrid scaffold with synthetic biomaterials and hydrogel using solid freeform fabrication technology." *Biofabrication* 3 (2011): 3.

52. Jinshu Mao, Swapna Kondu, Hai-Feng Ji, and Michael J. McShane. "Study of the Near-Neutral pH-Sensitivity of Chitosan/Gelatin Hydrogels by Turbidimetry and Microcantilever Deflection." *Biotechnology and Bioengeering* 95 .3 (2006): 333–341.

53. José M. Morachis, Enas A. Mahmoud, and Adah Almutairi. "Physical and Chemical Strategies for Therapeutic Delivery by Using Polymeric Nanoparticles." *Pharmacological Review* 64.3 (2012): 505–519.

54. Junmin Zhu, Roger E Marchant. "Design properties of hydrogel tissue-engineering scaffolds." *Expert Review of Medical Devices* 8.5 (2011): 607–626.

55. Kadari, Amrita, et al. "Design of multifunctional peptide collaborated and docetaxel loaded lipid nanoparticles for antiglioma therapy." *European Journal of Pharmaceutics and Biopharmaceutics* 132 (2018): 168-179.

56. Kuen Yong Lee, and David J. Mooney. "Alginate: properties and biomedical applications." *Progress in Polymer Science* 37.1 (2012): 106–126.

57. Kulseng, B., et al. " Transplantation of." *Transplantation* 67 (1999): 978–984.

58. Kyobula, Mary, et al. "3D inkjet printing of tablets exploiting bespoke complex geometries for controlled and tuneable drug release." *Journal of Controlled Release* 261 (2017): 207-215.

59. Lajoinie, A, et al. "Oral drug dosage forms administered to hospitalized children: Analysis of 117,665 oral administrations in a French paediatric hospital over a 1-year period." *International Journal of Pharmaceutics* 500 (2016): 336 - 344.

60. Lauretta M.S. Chana, Simon Lowesa, Barry H. Hirst. "The ABCs of drug transport in intestine and liver: efflux proteins." *European Journal of Pharmaceutical Sciences* 21 (2004): 25–51.

61. Lawson, Graham, John Ogwu and Sangeeta Tanna. "Quantitative screening of the pharmaceutical ingredient for the rapid identification of substandard and falsified medicines using reflectance infrared spectroscopy." *PLoS ONE* 13.8 (2018).

62. Leppert W, Zajczkowska R, Wordliczek J. "PATHOPHYSIOLOGY AND CLINICAL CHARACTERISTICS OF PAIN." *JOURNAL OF PHYSIOLOGY AND PHARMACOLOGY* 67.6 (2016): 787-799.

63. Li, Huijun, et al. "3D Bioprinting of Highly Thixotropic Alginate/Methylcellulose Hydrogel with Strong Interface Bonding." *Applied Materials and Interfaces* 9 (2017): 20086-20097.

64. Li, Man, et al. "pH-sensitive folic acid and dNP2 peptide dual-modified liposome for enhanced targeted chemotherapy of glioma." *European Journal of Pharmaceutical Sciences* 124 (2018): 240-248.

65. —. "Synergistic tumor microenvironment targeting and blood–brain barrier penetration via a pH-responsive dual-ligand strategy for enhanced breast cancer and brain metastasis therapy." *Nanomedicine: Nanotechnology, Biology, and Medicine* 14 (2018): 1833-1843.

66. Liang, X, et al. "Circumventing Tumor Resistance to Chemotherapy by Nanotechnology." *Methods Molecular Biology* 569 (2010): 467-488.

67. Lim, Seng Han, et al. "3D printed drug delivery and testing systems — a passing fad or the future?" *Advanced Drug Delivery Reviews* 132 (2018): 139-168.

68. Lindsey A Sharpe, Adam M Daily, Sarena D Horava, and Nicholas A Peppas. "Therapeutic applications of hydrogels in oral drug delivery." *Expert Opinion on Drug Delivery* 11.6 (2014): 901–915.

69. —. "Therapeutic applications of hydrogels in oral drug delivery." *Expert Opinion on Drug Delivery* 11.6 (2014): 901–915.

70. Long, Jingjunjiao, et al. "Application of Fused Deposition Modelling (FDM) Method of 3D Printing in Drug Delivery." *Current Pharmaceutical Design* 23 (2017): 433-439.

71. Lucia, Morelli. "Monitoring the Fate of Orally Administered PLGA." *Pharmaceutics* (2019): doi:10.3390/pharmaceutics11120658.

72. Maher, P S, et al. "Construction of 3D biological matrices using rapid prototyping technology." *Rapid Prototyping Journal* 15.3 (2009): 204-210.

73. Maksimenko, Olga, et al. "Doxorubicin-loaded PLGA nanoparticles for the chemotherapy of glioblastoma: Towards the pharmaceutical development." *International Journal of Pharmaceutics* 572 (2019).

74. Maleki, H, et al. "Methotrexate-Loaded PLGA Nanoparticles: Preparation, Characterization and their Cytotoxicity Effect on Human Glioblastoma U87MG cells." *International Journal of Medical Nano Research* 4.1 (2017): 1-9.

75. Malhotra, Meenakshi and Satya Prakash. "Targeted drug delivery accross the blood-brain-barrier using cell penetrating peptites tagged nanoparticles." *Current Nanoscience* 7 (2011): 81-93.

76. Marco Santoro, Alexander M. Tatara, and Antonios G. Mikosa. "GELATIN CARRIERS FOR DRUG AND CELL DELIVERY IN TISSUE ENGINEERING." *Journal of Cotrol Release* 28 (2015): 210–218.

77. Marta Szekalska, Agata Puciłowska, Emilia Szymańska, Patrycja Ciosek, and Katarzyna Winnicka. "Alginate: Current Use and Future Perspectives in Pharmaceutical and Biomedical Applications." *International Journal of Polymer Science* (2016): https://doi.org/10.1155/2016/7697031.

78. Martínez-Martínez, Mayte, et al. "Covalently crosslinked organophosphorous derivatives-chitosan hydrogel as a drug delivery system for oral administration of camptothecin." *European Journal of Pharmaceutics and Biopharmaceutics* 136 (2019): 174-183.

79. Masserini, Massimo. "Nanopartices for brain drug delivery." *ISRN Biochemistry* 2013:238428 (2013).

80. Maya Haus-Cohen, Yehuda G Assaraf, Liat Binyamin, Itai Benhar, Yoram Reiter. "Disruption of P-glycoprotein Anticancer Drug Efflux Activity by a Small Recombinant Single-Chain Fv Antibody Fragment Targeted to an Extracellular Epitope." *International Journal of Cancer* (2004): DOI: 10.1002/ijc.20037.

81. Mehata, Abhishesh Kumar, et al. "Trastuzumab decorated TPGS-g-chitosan nanoparticles for targeted breast cancer therapy." *Colloids and Surfaces B: Biointerfaces* 173 (2019): 366-3677.

82. Mira Jivraj, Luigi G. Martini and Carol M. Thomson. "An overview of the different excipients useful for the direct compression of tablets." *research focus* 3.2 (2000): 58-62.

83. Mooney, Jianyu Li and David J. "Designing hydrogels for controlled drug delivery." *Nature Reviews Materials* 1.12 (2016): 16071.

84. Muhammad Rizwan, Rosiyah Yahya, Aziz Hassan, Muhammad Yar, Ahmad Danial Azzahari, Vidhya Selvanathan, Faridah Sonsudin, and Cheyma Naceur Abouloula. "pH Sensitive Hydrogels in Drug DeliverBrief History, Properties, Swelling, and Release Mechanism, Material Selection and Applications." *Polymers* 9.4 (2017): 137.

85. Musmade, K P, et al. "Methotrexate-loaded biodegradable nanoparticles: preparation, characterization and evaluation of its cytotoxic potential against U-343 MGa human neuronal glioblastoma cells." *Bulletin of Material Science* 37.4 (2014): 945-951.

86. Naghieh, Saman, et al. "Influence of crosslinking on the mechanical behavior of 3D printed alginate scaffolds: Experimental and numerical approaches." *Journal of the Mechanical Behavior of Biomedical Materials* 80 (2018): 111-118.

87. Nakumara, Hidiye. "Direct permeation of nanoparticles across membranes: A Review ." *KONA Power and Particle Journal* 78 (2017): 1-16.

88. Natália Noronha Ferreira, Taciane Alvarenga Perez , Liliane Neves Pedreiro , Fabíola Garavello Prezotti , Fernanda Isadora Boni , Valéria Maria de Oliveira Cardoso , Tiago Venâncio , Maria Palmira Daflon Gremião. "A Novel pH-responsive Hydrogel-Based on Calcium Alginate Engineered by the Previous Formation of Polyelectrolyte Complexes (PECs) Intended to Vaginal Administration." *Drug Development and Industrial Pharmacy* (2017): DOI: 10.1080/03639045.2017.1328434.

89. Okwuosa, T C, et al. "On demand manufacturing of patient-specific liquid capsules via coordinated 3D printing and liquid dispensing." *European Journal of Pharmaceutical Sciences* 118 (2018): 134-143.

90. Oyen, Eneko Axpe and Michelle L. "Applications of Alginate-Based Bioinks in." *International Journal of Molecular Sciences* (2016): doi:10.3390/ijms17121976 .

91. Ozkan, T, et al. "Manufacturing Engineering Challenges of Pharmaceutical 3D Printing for on-Demand Drug Delivery." *Engineering Technology* 1.5 (2018).

92. Panupong Jaipan, Alexander Nguyen and Roger J. Narayan. "Gelatin-based hydrogels for biomedical applications." *MRS Communicatios* (2017): https://doi.org/10.1557/mrc.2017.92.

93. Parisa Ghasemiyeh, Soliman Mohammadi-Samani. "Hydrogels as Drug Delivery Systems; Pros and Cons." *Trends in Pharmaceutical Sciences* (2019): DOI 0.30476/TIPS.2019.81604.1002.

94. Park Heon, Nathan Gasek, Jaden Hwang, Daniel J. Weiss and Patrick C. Lee. "Effect of temperature on gelation and cross-linking of gelatin methacryloyl for biomedical applications." *Physics of Fluids* (2020): https://doi.org/10.1063/1.5144896.

95. Pawar , Vivek K, et al. "Improved chemotherapy against breast cancer through immunotherapeutic activity of fucoidan decorated electrostatically assembled nanoparticles bearing doxorubicin." *International Journal of Biological Macromolecules* 122 (2019): 1100-1114.

96. Pietrzak, Katarzyna, Abdullah Isreb and Mohamed A Alhnan. "A flexible-dose dispenser for immediate and extended release 3D printed tablets." *European Journal of Pharmaceutics and Biopharmaceutics* 96 (2015): 380-387.

97. Pleass, Winnifred Bertha. "Some physical conditions affecting the setting of gelatin and the bearing of the results on the theory of gel formation." *Proceedings of the Royal Society A* 126.802 (1930).

98. Prateek, Sehgal. "Fast Dissolving Tablets: A New Venture in Drug Delivery." *American journal of pharmatech research* 4.2 (2012): 2249-3387.

99. Preshita P.Desai, Abhijit A.Date, Vandana B.Patravale. "Overcoming poor oral bioavailability using nanoparticle formulations – opportunities and limitations." *Drug Discovery Today: Technologies* 2.9 (2012): 87-95.

100. Qi Xing, Keegan Yates, Caleb Vogt, Zichen Qian, Megan C. Frost & Feng Zhao. "Increasing Mechanical Strength of Gelatin Hydrogels by Divalent Metal Ion Removal." *Scientific Reports* (2014): DOI: 10.1038/srep04706.

101. Qiu Y, Park K. "Environment-sensitive Hydrogels for Drug Delivery." *Advance drug delivery review* (2001): DOI: 10.1016/s0169-409x(01)00203-4.

102. Rebecca L. Siegel, Kimberly D. Miller, Ahmedin Jemal DVM. "Cancer statistics." *ACS Journals* 66.1 (2016): 7-30.

103. Rezvantalab, S, et al. "PLGA-Based Nanoparticles in Cancer Treatment." *Frontiers in Pharmacology* 9 (2018).

104. Richard A. Walgren, Karl J. Karnaky, George E. Lindenmayer and Thomas Walle. "Efflux of Dietary Flavonoid Quercetin 4′-β-Glucoside across Human Intestinal Caco-2 Cell

Monolayers by Apical Multidrug Resistance-Associated Protein-2." *Journal of Pharmacology and Experimental Therapeutics* 3.294 (2000): 830-836.

105. Robert W. Robey, Kristen M. Pluchino, Matthew D. Hall, Antonio T. Fojo, Susan E. Bates, and Michael M. Gottesman. "Revisiting the role of efflux pumps in multidrug-resistant cancer." *Nature Review Cancer* 18.7 (2019): 452–464.

106. Ruiz-Gatón, Luisa, et al. "Pegylated poly(anhydride) nanoparticles for oral delivery of docetaxel." *European Journal of Pharmaceutical Sciences* 118 (2018): 165-175.

107. Saha P, Saarai A, Kasparkovaac V, Sedlacek T. "On the development and characterisation of crosslinked sodium alginate/gelatine hydrogels." *Journal of the Mechanical Behavior of Biomedical Materials* 18 (2013): 152-166.

108. Santos de Laia, Andréia Grossi, Ezequiel de Souza Costa Júnior and Hermes de Souza Costa. "A study of sodium alginate and calcium chloride interaction through films for intervertebral disc regeneration uses." *21º CBECIMAT - Congresso Brasileiro de Engenharia e Ciência dos Materiais*. Cuiabá, MT, Brasil, 2014. 7341 - 7348.

109. Sara Salatin, and Ahmad Yari Khosroushahi. "Overviews on the cellular uptake mechanism of polysaccharide colloidal nanoparticles." *Journal of Cellular and Molecular Medicine* 21.9 (2017): 1668–1686.

110. Sardo, Hossein Shahdadi, et al. "A review on 5-aminosalicylic acid colon-targeted oral drug delivery systems." *International Journal of Pharmaceutics* 558 (2019): 367 - 379.

111. Sayantan Ray, Mathew Joy,Biswanath S,Swapankumar Ghosha. "pH dependent chemical stability and release of." *RSC Advances* 5 (2015): 39482.

112. Schütz, Kathleen, et al. "Three-dimensional plotting of a cell-laden alginate/ methylcellulose blend: towards biofabrication of tissue engineering constructs with clinically relevant dimensions." *Journal of Tissue Engineering and Regenerative Medicine* 11 (2017): 1574-1587.

113. Seabury, S A, et al. "The impact of self- and physician-administered cancer treatment on work productivity and healthcare utilization." *Research in Social and Administrative Pharmacy* 14 (2018).

114. Sendra, M, et al. "Cytotoxicity of CeO2 nanoparticles using in vitro assay with Mytilus galloprovincialis hemocytes: Relevance of zeta potential, shape and biocorona formation." *Aquatic Toxicology* 200 (2018): 13-20.

115. Shahed Behzadi, Vahid Serpooshan,Wei Tao,Majd A. Hamaly,Mahmoud Y. Alkawareek,Erik C. Dreaden,Dennis Brown,Alaaldin M. Alkilany,Omid C. Farokhz. "Cellular Uptake of Nanoparticles: Journey Inside the Cell." *Chemical Society Reviews* (2018): doi: 10.1039/c6cs00636a.

116. Shen, Ming-Yin, et al. "Hierarchically targetable polysaccharide-coated solid lipid nanoparticles as an oral chemo/thermotherapy delivery system for local treatment of colon cancer." *Biomaterials* 197 (2019): 86 - 100.

117. Shi, Kejing, et al. "Drop-On-Powder 3D Printing of Tablets with an Anti-Cancer Drug, 5-Fluorouracil." *Pharmaceutics* 150.11 (2019).

118. Shin, Jung Hwal and Hyun-Wook Kang. "The Development of Gelatin-Based Bio-Ink for Use in 3D Hybrid Bioprinting." *International Journal of Precision Engineering and Manufacturing* 19.5 (2018): 767-771.

119. Shrawani Lamichhane, Santosh Bashyal, Taekwang Keum, Gyubin Noh, Seo Jo, Eun Rakesh, Bastola Choi, Jaewoong Sohn, Dong Hwan, Lee Sangk. "Complex formulations, simple techniques: Can 3D printing technology be the Midas touch in pharmaceutical industry?" *Asian Journal of Pharmaceutical Sciences* 14.5 (2019): 465-479.

120. Siegel, Hirenkumar K. Makadia and Steven J. "Poly Lactic-co-Glycolic Acid (PLGA) as Biodegradable Controlled Drug Delivery Carrier." *Polymers* 3.3 (2011): 1377-1399.

121. —. "Poly Lactic-co-Glycolic Acid (PLGA) as Biodegradable Controlled Drug Delivery Carrier." *Polymers* 3.3 (2011): 1377-1397.

122. —. "The Poly Lactic-co-Glycolic Acid (PLGA) as Biodegradable." *Polymers* 3 (2011): 1377-1397.

123. Simsek, Soner, et al. "Brain targeting of Atorvastatin loaded amphiphilic PLGA-b-PEG nanoparticles." *Journal of Microencapsulation* 30.1 (2013): 10-20.

124. Sohail, Muhammad Farhan, et al. "Advancements in the oral delivery of Docetaxel: challenges, current state-of-the-art and future trends." *International Journal of Nanomedicine* 13 (2018): 3145-3161.

125. Solanki, Nayan G, et al. "Formulation of 3D Printed Tablet for Rapid Drug Release by Fused Deposition Modeling: Screening Polymers for Drug Release, Drug-Polymer Miscibility and Printability." *Journal of Pharmaceutical Sciences* 107 (2018): 390-401.

126. Son, Geun Hyung Kim and Joon Gon. "3D polycarprolactone (PCL) scaffold with hierarchical structure fabricated by a piezoelectric transducer (PZT)-assisted bioplotter." *Applied Physics* 94 (2009): 781–785.

127. Sosnik, Alejandro. "Alginate Particles as Platform for Drug Delivery by the Oral route: State-of-the-Art." ISRN Pharmaceutics, 2014.

128. Stodghill, Steven P. "Thermal Analysis – A Review of Techniques and Applications in the Pharmaceutical Sciences." *American Pharmaceutical Review* 13.12 (2010).

129. Stones, James and Catherine Jewell. "3D printing of pharmaceuticals: patent and regulatory challenges." *Pharmaceutical Patent Analyst* 6 (2017).

130. Sudipta Senapati, Arun Kumar Mahanta, Sunil Kumar & Pralay Maiti. "Controlled drug delivery vehicles for cancer treatment and their performance." *Signal Transduction and Targeted Therapy* (2018): https://doi.org/10.1038/s41392-017-0004-3.

131. Sudipta Senapati, Arun Kumar Mahanta, Sunil Kumar, and Pralay Maiti. "Controlled drug delivery vehicles for cancer treatment and their performance." *Signal Transduct Target Therapy* 3 (2018): 7.

132. Sulin Zhang, Huajian Gao, and Gang Bao. "Physical Principles of Nanoparticle Cellular Endocytosis." *Nano Letters* 22.9 (2015): 8655–8671.

133. Sun, Seung-Joon Song Jaesoon Choi Yong-Doo Park Soyoung Hong Jung Joo Lee Chi Bum Ahn Hyuk Choi Kyung. "Sodium Alginate Hydrogel-Based Bioprinting Using a Novel Multinozzle Bioprinting System." *Artificial Organs* 35.11 (2011): 1132-1136.

134. Taira, Noriko, et al. "Electrochemical printing of calcium alginate/gelatin hydrogel." *Electrochimica Acta* 281 (2018): 429-436.

135. Tan, K X, et al. "Towards targeted cancer therapy: Aptamer or oncolytic virus?" *European Journal of Pharmaceutical Sciences* 96 (2017): 8-19.

136. Tariq, Ubaid and Mohamed Mazhar. "Three dimensional (3D) drug printing: A revolution in Pharmaceutical Science." *PharmaTutor* 7.3 (2019): 19-25.

137. Ternik, Robert, et al. "Assessment of swallowability and palatability of oral dosage forms in children: Report from an M-CERSI pediatric formulation workshop." *International Journal of Pharmaceutics* 536 (2018): 570 - 581.

138. Trenfield, Sarah J, et al. "3D Printing Pharmaceuticals: Drug Development to Frontline Care." *Trends in Pharmacological Sciences* 39.5 (2018): 440 - 451.

139. Wan , Xiaoang, et al. "Assessing the expectations associated with pharmaceutical pill colour and shape." *Food Quality and Preference* 45 (2015): 171-182.

140. Wang, G, et al. "Controlled preparation and antitumor efficacy of vitamin E TPGS-functionalized." *International Journal of Pharmaceutics 446* 446 (2013): 24 - 33.

141. Wang, Xiaohong, et al. "Gelatin-Based Hydrogels for Organ 3D Bioprinting." *Polymers* 9.401 (2017).

142. Weinberg. *The biology of cancer*. Garland science, 2013.

143. WHO. "Cancer." 2020. *World Health Organisation.* 2020. <https://www.who.int/health-topics/cancer>.—. "Global Health Observatory. Geneva: World Health Organization." 2018.

144. Widemann B C, Adamson P C. "Understanding and managing methotrexate nephrotoxicity." *The oncologist* 11.6 (2006): 694-703.

145. Xu, Yining, et al. "An overview of in vitro, ex vivo and in vivo models for studying the transport of drugs across intestinal barriers." *Advanced Drug Delivery Reviews* 175 (2021).

146. Yang YY1, Chung TS, Ng NP. "Morphology, drug distribution, and in vitro release profiles of biodegradable polymeric microspheres containing protein fabricated by double-emulsion solvent extraction/evaporation method." *Biomaterials* 44.3 (2001): 231-41.

147. Yang, F, et al. "Bioavailability Enhancement of Paclitaxel via a Novel Oral Drug Delivery System: Paclitaxel-Loaded Glycyrrhizic Acid Micelles." *Molecules* 20 (2015): 4337-4356.

148. Yu Zhao, Yang Li, Shuangshuang Mao, Wei Sun and Rui Yao. "The influence of printing parameters on cell survival rate and printability in microextrusion-based 3D cell printing technology." *Biofabrication* 7 (2015): 1-11.

149. Yuandong Ma, Yi Zheng, Kexin Liu, Ge Tian, Yan Tian, Lei Xu, Fei Yan, Laiqiang Huang, and Lin Mei. "Nanoparticles of Poly(Lactide-Co-Glycolide)-d-a-Tocopheryl Polyethylene Glycol 1000 Succinate Random Copolymer for Cancer Treatment." *Nanoscale Research Letters* 5 (2010): 1161–1169.

150. Yung, Haizheng Zhao Lin Yue Lanry. "Addition of TPGS to folate-conjugated polymer micelles for selective tumor targeting." *Society of biomaterial* 91.2 (2008): 505-518.

151. Yuqing Gong, Pallabita Chowdhury, Prashanth K. B. Nagesh, Mohammad A. Rahman. “Freddie Bray BSc, MSc, PhD Jacques Ferlay ME Isabelle Soerjomataram, Rebecca L. Siegel, Lindsey A. Torre, Ahmedin Jemal.” *ACS* 68.6 (2018): 394-424.